Modeling acto-myosin interaction: beyond the Huxley–Hill framework

Louis-Pierre Chaintron, Matthieu Caruel, François Kimmig

MathematicS In Action
Version de travail

Modeling acto-myosin interaction : beyond the Huxley–Hill framework

Louis-Pierre Chaintron
Matthieu Caruel
François Kimmig

[*] DMA, École Normale Supérieure 45 rue d'Ulm, 75005 Paris, France; Inria – LMS, École polytechnique, CNRS – Institut Polytechnique de Paris; Palaiseau, France.
Email address: louis-pierre.chaintron@ens.psl.eu
[†] Univ Paris Est Creteil, Univ Gustave Eiffel, CNRS, UMR 8208, MSME, F-94010 Créteil, France.
Email address: matthieu.caruel@u-pec.fr
[‡] Inria; LMS, École polytechnique, CNRS – Institut Polytechnique de Paris; Palaiseau, France.
Email address: francois.kimmig@inria.fr.

Abstract. Contractile force in muscle tissue is produced by the interaction of myosin molecular motors that bind and pull on specific sites located on surrounding actin filaments. The classical framework set by the landmark works of A.F. Huxley and T.L. Hill to model this active system is build on the central assumption that thermal fluctuations of a given myosin motor are sufficiently small so that it cannot interact with more than one binding site at any time. In this paper we present the physiological and mathematical limitations of this approach to motivate a new formulation that circumvent them without resorting to the more complex multi-site model paradigm.

The acto-myosin system is now described as a Markov process combining Langevin drift-diffusion and Poisson jumps dynamics. We show that the corresponding system of Stochastic Differential Equation is well-posed and derive its Partial Differential Equation analog in order to obtain the thermodynamic balance laws. We finally show that by applying standard elimination procedures, a modified version of the original Huxley-Hill framework can be obtained as a reduced version of our model. Theoretical results are supported by numerical simulations where the model outputs are compared to benchmark experimental data.

Contents

Keywords: Applied mathematics, Applied probability, Muscle contraction, Thermodynamics, Molecular motors, Jump-diffusion process, Poisson random measures.
2020 *Mathematics Subject Classification:* 00X99.

1. Introduction

1.1. Muscle contraction

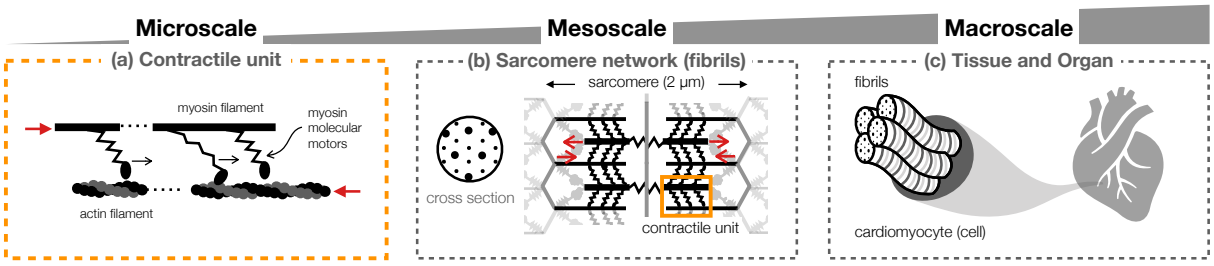

Figure 1. Physiological context. (a) The muscle contraction is generated by the interaction of myosin molecular motors with actin filaments in so-called contractile units. (b) Antagonist contractile units are stacked in parallel to form sarcomeres. (c) sarcomere are assembled in series to form the fibrils of the muscle cells.

Muscle contraction is produced at the nanoscale by the concerted action of myosin molecular motors, converting metabolic energy into mechanical power. These motors are proteins called myosins that act as enzymes catalyzing the hydrolysis of ATP[1] in the presence of another protein, call f-actin with which myosin motors interact to form so-called cross-bridges. In the muscle tissue, at the microscale, myosins form thick filaments running in the longitudinal direction of the muscle fibers, see Figure 1(a). F-actin also takes the form of filaments made out of polymerized g-actin (globular actin) which runs parallel to the mysoin filaments.

The metabolic energy extracted from the hydrolysis of ATP by the motors is transformed into a mechanical working strokes that pull on the actin filament. Both filaments are oriented to build a contractile unit as the myosin-actin interaction produces their relative sliding in opposite direction

At the mesoscale, antagonists contractile units are stacked in the transverse direction and form a $\sim 2\,\mu$m-long sarcomere, see Figure 1(b). Sarcomere themselves are arranged in series to form bundles of fibrils inside the muscle cells, see Figure 1(c). Thanks to this highly organized

[1]Adhenosine TriPhosphate

structure, the metabolic activity of the acto-myosin molecular system results in the macroscopic contraction.

At the core of the contraction mechanism is the interaction between a myosin protein and its neighboring actin monomers. This interaction takes the form of a cyclic succession of structural and chemical transitions during which a myosin binds actin to form a force producing cross-bridge, and then disengage to hydrolyze one ATP molecule, see [25] for more details on the molecular mechanism. The constant supply of fresh ATP molecule is necessary to maintain this cycle out of equilibrium.

1.2. **Modeling the actin-myosin interaction**

The first physiologically relevant theory of actin-myosin interaction was formulated in 1957 by A.F. Huxley [27]. The general idea, which is developed in details in the next section, was to model a representative myosin protein as a linear elastic spring existing in two states: attached to actin or detached. Huxley postulated the existence of specific target zones (or binding sites) positioned periodically on the actin filament. While the myosin is bound, the tension it generates is proportional to the distance between the tip (head) of the protein which is located at the binding site and its anchor in the myosin filament. The attachment and detachment events are modeled as a "chemical" jump process with rates that depend on the distance to the nearest binding site. The dynamics of the system takes the form of a transport PDE for the population of attached and detached myosins, with sources and sinks terms accounting for the transition between the two states.

This modeling framework has been formalized and generalized by T.L. Hill and co-workers [24, 22, 23, 14, 15]. The generalization consisted in formulating the population dynamics equations for an arbitrary number of states and in formalizing the fundamental mathematical requirements that ensure the compatibility of the model with conservation laws and in particular, the thermodynamic principles.

Since then plethora of such chemical-mechanical models have been proposed to account for a constantly increasing body of experimental data. The refinements as compared to the original two-state model of Huxley consists in defining additional chemical states and the corresponding transition rates, see for instance [28, 47, 52, 53, 11, 54, 51, 2, 38, 39, 41] or in using generalized non-linear energy potentials for the elastic spring representation of the myosin head [45, 31].

The goal of this paper is to revisit one of the fundamental hypothesis underlying all Huxley–Hill-like models, while proposing a new SDE formulation, based on Poisson random measures.

1.3. **The Huxley'1957 model**

Before presenting the objectives of our work, we here summarize the framework set by the landmark Huxley'1957 model (H57 model).

The framework. The original Huxley model [27] sets a 1D framework to describe the dynamics of a population of independent myosin motors interacting with a single actin filament, see Figure 1(a). Since the motors are considered independent, considering a single representative motor is sufficient, see Figure 2(a). We define as the origin of the 1D axis, the position of a representative myosin anchor point to the myosin filament. The actin sites are located on the actin filament, supposed to be rigid and parallel to the myosin filament. At all time, the myosin head has the possibility to bind *only* to the nearest actin site whose position, with respect to the anchor point, is parametrized by the variable s.

The distance between consecutive binding sites being denoted by d, the binding to the nearest site occurs necessarily within the restricted *fixed* window $(-d/2, +d/2)$ so that the current actin site is at most $d/2$ far from this base point: a site enters the window at the time the previous one leaves.

The myosin head is assumed to attach instantaneously to its site with rate $f(s)$ to form a cross-bridge. This cross-bridge can subsequently be detached, also instantaneously, with rate $g(s)$. Both rates $f(s)$ and $g(s)$ are assumed to depend only on s.

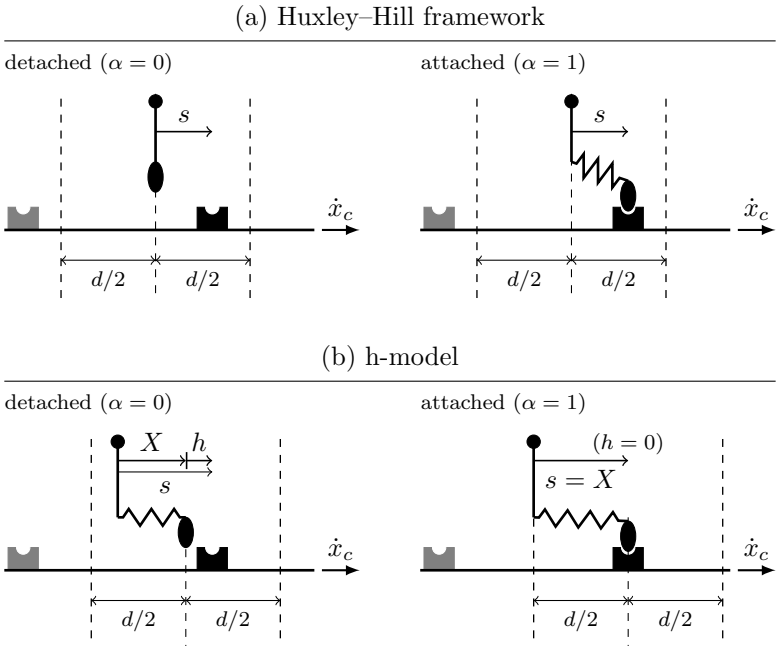

Figure 2. (a) The Huxley–Hill model is parametrized by the distance s separating the myosin anchor from its nearest binding site. The distance between two consecutive sites is denoted by d. After attachment, the formed cross-bridge is represented as a spring of length s. (b) The h-model considers the position of the detached myosin head X relative to the same anchor point. The nearest binding site is now defined relative to the position of the head and parametrized by the variable h.

During the contraction, the actin filament slides relative to the myosin filament with an *imposed* velocity $\dot{x}_c(t)$. In this point of view, the molecular motor produces a force as a response to an input sliding velocity.

Classical formulation. Let $\alpha \in \{0, 1\}$ denote the attachment state of the myosin head: $\alpha = 0$ stands for a detached configuration, while $\alpha = 1$ means the myosin head is attached to the actin site located at distance s of the myosin anchor point. The original Huxley model was concerned with the *conditional* probability $P_\alpha(s, t)$ for the head being in the configuration α knowing the location s of the closest actin site at time t. At any given s, mass conservation imposes that $P_0(s, t) + P_1(s, t) = 1$, since the state α is either 0 or 1, indeed. It is possible to describe the population dynamics using a PDE system: the sliding velocity gives a transport term, while the jump mechanisms with rates $f(s)$ and $g(s)$ are given by linear terms [27]:

$$\begin{cases} \partial_t P_1(s,t) + \dot{x}_c(t)\partial_s P_1(s,t) = -g(s)P_1(s,t) + f(s)\left[1 - P_1(s,t)\right], & (1.1) \\ P_0(s,t) = 1 - P_1(s,t). & (1.2) \end{cases}$$

Notice that the compatibility of the model (1.1) with the principles of thermodynamics is not guarantied *a priori* since the rates f and g may not satisfy the detailed balance condition. This problem was solved in the extension of the model proposed by T.L. Hill and co-workers, see the next section for more details. Hence, the terminology *Huxley–Hill framework*.

1.4. **Limits of the Huxley formulation**

The Huxley–Hill framework suffers from a series of inherent limitations. These limitations are all consequences of the essential assumption made that a myosin head can interact only with the nearest binding site located in a *fixed* window of length d.

In the structural representation of the actin-myosin interaction, the detached myosin head fluctuates, and therefore the probability to form a cross-bridge with a nearby site depends on

the capacity for the myosin molecular structure to sufficiently deform to reach this site. Hence, the assumption that only one site can be bound by the myosin head within a given window of length d supposes that the maximal extension of the cross-bridge is less than $d/2$. If the characteristic length of the fluctuations remains small compared to the inter-site distance, the probability for a given head to interact with a site that is not the closest to its anchor point can be neglected, indeed.

This representation has the following consequences on the rates $f(s)$ and $g(s)$ appearing in (1.1).

(1) Attachment is not permitted on the borders of the interval. Since the deformation of the protein is assumed to be less than $d/2$, attachment can't occur when s equals the "boundary points" (i.e. $-d/2$ or equivalently $+d/2$), imposing that

$$f(-d/2) = f(+d/2) = 0$$

It would make sense to consider $f(s)$ being continuous and spiked around $s = 0$, and identically being 0 when s is close enough to the borders.

(2) Detachment is compulsory on the borders of the interval. The site can't be located at the boundary points during in the attached configuration since this would imply a jump of the cross-bridge from one side of the window to the other one, which is obviously non-physical. The distance d being (strictly) larger than the cross-bridge maximal extension, this situation has to be excluded by enforcing at least

$$\lim_{\substack{s\to -d/2 \\ s>-d/2}} g(s) = \lim_{\substack{s\to +d/2 \\ s<+d/2}} g(s) = +\infty$$

with an imposed discontinuity at the boundary point.

The physiological limitations of the Huxley–Hill framework are thus related to the structural organization of the system. The actin filament is a double-stranded helix of globular monomers whose diameter is about 5.5 nm. The long periodicity of actin corresponds to 7 of these monomers [17]. At rest the regulatory units are covered by a calcium sensitive protein called tropomyosin. Upon activation, the calcium ions that are released in the cell bind to troponin-tropomyosin complex, which triggers a conformational change that uncovers the actin monomers, making them available for attachment by myosin. Experimental studies on single molecules suggested that only few (possibly 3) monomers are correctly oriented to enable strong attachment, once every ∼40 nm. Therefore, several models propose that the binding event can occur only on so-called "target zones" separated by a distance of $d \approx 40\,\mathrm{nm}$ [43, 55]. Other models, however, postulate that the interval between the binding site correspond to the monomer repeat of 5.5 nm, [47, 2]. While this may not be the case in situ, it is realistic for in vitro acto-myosin preparation where regulatory proteins are removed [45].

The elastic constant of the attached myosin protein has been evaluated at $\kappa \approx 1\,\mathrm{pN\,nm^{-1}}$ [4], which correspond to thermal fluctuations of about $\sqrt{\pi k_b T/\kappa} \approx 3.6\,\mathrm{nm}$. One also has to consider that the myosin motor can undergo conformational change as large as 10 nm [25, 50].

From the point of view of the detached state, given the above estimations, one can infer that with an actin periodicity of $d = 40\,\mathrm{nm}$, the probability for a given head to travel $d/2 \approx 20\,\mathrm{nm}$ can indeed be neglected. However, if one considers a periodicity of $d = 5.5\,\mathrm{nm}$, then the probability for a given head to reach a remote site has to be considered. Furthermore, recent studies that use a non-linear elastic models for the attached motors predict that the cross-bridges can remain formed along distances up to 50 nm, see [40, 42], which makes the Huxley–Hill framework not appropriate from the point of view of the attached state. In a nutshell, the Huxley–Hill framework is reasonable if the assumption $d = 40\,\mathrm{nm}$ is taken and that long cross-bridge extensions are prevented but is not adapted otherwise.

To circumvent these issues, the original Huxley model has been extended by Hill and co-workers to include the possibility to bind multiple sites from the same detached state [22]. This approach requires defining new rate functions, which makes the calibration of the models more difficult, and potentially less robust to the variability in the experimental data.

In this paper, we propose an alternative and less-complex approach to lift the aforementioned limitations by reconsidering the initial assumptions setting the Huxley–Hill framework to overcome these limitations, see Figure 2(b). Our h-model is based on the following assumptions.

(1) A myosin head is parametrized by the position x of its head with respect to its anchor point on the myosin filament.

(2) The position of the nearest actin binding site is not defined with respect to the anchor point anymore but instead with respect to the position of the head x. This relative position is denoted by h.

(3) A given myosin head can bind only to the nearest actin site.

We formulate the h-model as a stochastic Markov process involving continuous Langevin dynamics for the position of the head and a discrete Poisson dynamics for the state (attached or detached). Throughout the paper, we will use two approaches to describe the system: a stochastic approach based on Stochastic Differential Equations and a deterministic approach based on Partial Differential Equations.

The results of this work are presented as follows. In Section 2, we reformulate the Huxley–Hill model (1.1) in order to introduce both approaches. The h-model itself is presented in Section 3. For both Huxley–Hill and h-model, we prove the compatibility with the thermodynamic principles. We will then show in Section 4 that the Huxley–Hill model can in fact be viewed as an analog of a reduced version of the h-model – the h-reduced model – obtained by asymptotic elimination of the variable x and h. Again, both formulations are presented and the compatibility with the thermodynamic principles is tracked. Finally, numerical illustrations of the h-model and its reduced version are presented in Section 5, where we compare the steady state properties of the models with benchmark experimental data characteristic of the mechanical performance of cardiac cells.

2. SDE formulation of the Huxley–Hill model using random measures

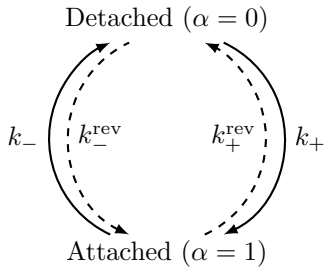

Figure 3. Schematic of the two state actin-myosin interaction cycle.

We start by building a Stochastic Differential Equation (SDE) representation for this system, defining a stochastic process whose law at given s will satisfy equation (1.1). More than giving a Lagrangian (particle) interpretation of the Huxley PDE system, this will permit simple Monte-Carlo simulations of this system (see Appendix A) without using heavy PDE solvers. This approach also paves the way for the incoming h-model, whose SDE interpretation will be more natural than its PDE one. The dynamics can be formalized as a càdlàg Markov process

$$(\alpha_t, s_t) \in \{0, 1\} \times \mathbb{T}_d \, , \, t \geq 0$$

the actin site being s_t and the state α_t standing for the current configuration (attached: $\alpha_t = 1$, or detached: $\alpha_t = 0$) of the cross bridge.

The variable s_t is the location of the nearest actin site, as well as it is the algebraic distance of this site to the base point, since the window and the coordinate axe originate at the same base point. It is therefore relevant to consider s_t as a continuous variable evolving in the one-dimensional torus $\mathbb{T}_d$ of center 0 and diameter d, which can be identified to the closed interval

$[-d/2, +d/2]$ with periodic boundary conditions: in this representation, the base point is the center 0 of the torus.

The s_t dynamics is then only translation with speed $\dot{x}_c(t)$, while α_t describes a jump process involving two states. The Hill thermodynamic analysis [22] of this model requires to split the global jump rates f and g appearing in (1.1) into four intermediary rates (see Section 2.1 for details on the purpose of this). They correspond to four Poisson jump events with state-dependent rates (see Figure 3).

- A direct attachment $0 \to 1$ with rate $k_+(s)$.
- A reverse jump $1 \to 0$ with rate $k_+^{\mathrm{rev}}(s)$.
- A direct detachment $1 \to 0$ with rate $k_-(s)$.
- A reverse jump $0 \to 1$ with rate $k_-^{\mathrm{rev}}(s)$.

These rates can be linked to the previous ones appearing in (1.1) by

$$f(s) = k_+(s) + k_+^{\mathrm{rev}}(s) \qquad g(s) = k_-(s) + k_-^{\mathrm{rev}}(s).$$

These jumps induce càdlàg (right-continuous with left limit) discontinuities, so that $\alpha_t = 1 - \alpha_{t^-}$ at the jump time t. This can be formalized using four independent Poisson random measures (see appendix A for reminders on this notion): $N_+(\mathrm{d}t, \mathrm{d}u)$, $N_+^{\mathrm{rev}}(\mathrm{d}t, \mathrm{d}u)$, $N_-(\mathrm{d}t, \mathrm{d}u)$ and $N_-^{\mathrm{rev}}(\mathrm{d}t, \mathrm{d}u)$ on $\mathbb{R}_+ \times \mathbb{R}_+$ with intensity measure $\mathrm{d}t \otimes \mathrm{d}u$. The u parameter in these measures accounts for the detachment rates. Finally, the dynamics of (α_t, s_t) can be represented by the SDE system:

$$\begin{cases} \mathrm{d}\alpha_t = (1-\alpha_{t^-}) \int_{\mathbb{R}_+} (1-2\alpha_{t^-})\, \mathbb{1}_{u \le k_+(s_t)} N_+(\mathrm{d}t, \mathrm{d}u) + \alpha_{t^-} \int_{\mathbb{R}_+} (1-2\alpha_{t^-})\, \mathbb{1}_{u \le k_+^{\mathrm{rev}}(s_t)} N_-(\mathrm{d}t, \mathrm{d}u) \\ \qquad\quad + \alpha_{t^-} \int_{\mathbb{R}_+} (1-2\alpha_{t^-})\, \mathbb{1}_{u \le k_-(s_t)} N_+(\mathrm{d}t, \mathrm{d}u) + (1-\alpha_{t^-}) \int_{\mathbb{R}_+} (1-2\alpha_{t^-})\, \mathbb{1}_{u \le k_-^{\mathrm{rev}}(s_t)} N_-(\mathrm{d}t, \mathrm{d}u), \\ \mathrm{d}s_t = \dot{x}_c(t)\mathrm{d}t \qquad \text{in } \mathbb{T}_d. \end{cases} \tag{2.1}$$

The pre-factors α_t and $1 - \alpha_t$ alongside the system allow to select which transition occurs or not depending on the value of $\alpha_t \in \{0, 1\}$; $\mathbb{1}_{\alpha_t=1}$ and $\mathbb{1}_{\alpha_t=0}$ could be written instead. Note that $1 - 2\alpha_{t^-}$ is always the jump amplitude when α_t jumps from a state to the other one (either for $0 \to 1$ or $1 \to 1$). When $\alpha_{t^-} = 0$, the N_+ and N_-^{rev} term in the SDE has a non-zero pre-factor, allowing an increment for α_t of $1 - 2\alpha_{t^-} = 1$. The same holds with an increment -1 when $\alpha_{t^-} = 1$ with the N_- and N_+^{rev} term.

Well-posedness for the SDE system (2.1) is a simple task (see references in appendix A) provided x_c is C^1 and coefficients k_+, k^{rev}, k_- and k_-^{rev} are Lipschitz – however this property is unclear in the Huxley–Hill framework, because rates must explode on the border of the window (see explanations in introduction).

The pathwise law p of the process belongs to the space $\mathcal{P}(D(\mathbb{R}_+, \{0,1\} \times \mathbb{T}_d))$ of probability measures on the Skorokhod space $D(\mathbb{R}_+, \{0,1\} \times \mathbb{T}_d)$ of càdlàg trajectories. The related t-marginal $p_t \in \mathcal{P}(\{0,1\} \times \mathbb{T}_d)$ is the joint law of (α_t, s_t) at time t: it is a probability measure $p_t(\mathrm{d}\alpha, \mathrm{d}s) = p_t(\alpha, \mathrm{d}s)\,\mathrm{d}\alpha$ on the state space $\{0,1\} \times \mathbb{T}_d$ ($\mathrm{d}\alpha = \delta_0 + \delta_1$ is the canonical mass measure on {0,1}). The law $p_t^s(\mathrm{d}s)$ of s_t at time t is the s-marginal of $p_t(\mathrm{d}\alpha, \mathrm{d}s)$ which can be defined by integrating over α:

$$p_t^s(\mathrm{d}s) = p_t(0, \mathrm{d}s) + p_t(1, \mathrm{d}s). \tag{2.2}$$

It satisfies the transport equation

$$\partial_t p_t^s + \dot{x}_c(t) \partial_s p_t^s = 0. \tag{2.3}$$

By transport, if s_0 is uniformly distributed at time $t = 0$, *it will be the case for s_t at every time* $t \ge 0$. This assumption shall now be made, so that

$$p_t(\mathrm{d}\alpha, \mathrm{d}s) = P_\alpha(s,t)\mathrm{d}\alpha \frac{\mathrm{d}s}{d}, \tag{2.4}$$

where $P_\alpha(s,t)$ is the conditional probability for a myosin motor, whose nearest site is located at s to be in state α. The α-marginal of $p_t(\mathrm{d}\alpha, \mathrm{d}s)$ conditionally on $s_t = s$ reads

$$\frac{p_t(\alpha, s)\,\mathrm{d}\alpha}{p_t(0,s) + p_t(1,s)} = \frac{P_\alpha(s,t)/d}{1/d}\mathrm{d}\alpha = P_\alpha(s,t)\mathrm{d}\alpha \tag{2.5}$$

The conditional law $P_\alpha(s,t)\mathrm{d}\alpha$ is a probability measure, and the normalization relation holds

$$P_0(s,t) + P_1(s,t) = 1, \tag{2.6}$$

making $P_\alpha(s,t)$ the remaining unknown.

Remark on notations. In the sequel, conditional probabilities will always be written with capital letters P, while normal case p will denote joint probabilities. Later we will also introduce reduced probabilities, which will be distinguished from the joint probabilities by a bar $\overline{p}$.

The time-evolution of p_t can be captured using regular test functions $\varphi : \{0,1\} \times \mathbb{T}_d \to \mathbb{R}$, which are called "observables". The infinitesimal generator (see [35]) L of this Markov process is an unbounded linear operator defined as

$$\frac{\mathrm{d}}{\mathrm{d}t}\mathbb{E}\left[\varphi(\alpha_t, s_t)\right] = \mathbb{E}\left[L\varphi(\alpha_t, s_t)\right]$$

for regular functions φ for which the derivative makes sense. This is the backward Kolmogorov equation; since (α_t, s_t) solves an SDE, this can be recovered using Ito's formula. In terms of p_t, this reads for any observable φ

$$\int_{\{0,1\}\times\mathbb{T}_d} \varphi\,\mathrm{d}\left(\partial_t p_t\right) = \int_{\{0,1\}\times\mathbb{T}_d} L\varphi\,\mathrm{d}p_t$$

If L admits an adjoint operator $L^\star$ on a subdomain of $\mathcal{P}\left(\{0,1\}\times\mathbb{T}_d\right)$, the related dual equation reads in the measure (weak) sense

$$\partial_t p_t = L^\star p_t.$$

This is the forward Kolmogorov equation (or the well-known Fokker-Planck equation in a diffusion setting); this is usually obtained integrating by parts. It is a strong PDE when the law admits a density $p_t(\mathrm{d}x, \mathrm{d}\alpha) = p_t(x,\alpha)\,\mathrm{d}x\mathrm{d}\alpha$.
The generator can be obtained following the derivation in section A. To a jump $0 \to 1$ correspond a rate $k_{0\to1}(\alpha, s) = \mathbb{1}_{\alpha=0} f(s)$ and a jump law $K_{0\to1}\left((\alpha,s), (\mathrm{d}\alpha', \mathrm{d}s')\right) = \delta_{1-\alpha}(\mathrm{d}\alpha')\,\delta_s(\mathrm{d}s')$ (δ is a Dirac measure, the location after jump being chosen here in a deterministic way), adding the term

$$k_{0\to1}(\alpha,s)\int_{\{0,1\}\times\mathbb{T}_d}\left[\varphi(\alpha',s') - \varphi(\alpha,s)\right]K_{0\to1}\left((\alpha,s), \left(\mathrm{d}\alpha', \mathrm{d}s'\right)\right) \\ = \mathbb{1}_{\alpha=0} f(s)\left[\varphi(1-\alpha,s) - \varphi(\alpha,s)\right]$$

to the total generator (in the rest of this article, jump measures won't be that much detailed: only non-deterministic jumps will be written to avoid heavy expressions); the prime variables denote the new values after jumps. The same holds for the $1 \to 0$ jumps. Summing these contributions and the transport term eventually gives

$$L\varphi(\alpha,s) = \dot{x}_c(t)\partial_s\varphi(\alpha,s) \\ + \mathbb{1}_{\alpha=0} f(s)\left[\varphi(1-\alpha,s) - \varphi(\alpha,s)\right] + \mathbb{1}_{\alpha=1} g(s)\left[\varphi(1-\alpha,s) - \varphi(\alpha,s)\right]. \tag{2.7}$$

Appendix A now provides the dual generator of each jump. The dual of the transport term in (2.7) is moreover given by straightforward integration by parts. Gathering everything leads to the dual operator $L^\star$ and the related equation:

$$\partial_t p_t(\alpha, \mathrm{d}s) + \dot{x}_c(t)\partial_s p_t(\alpha, \mathrm{d}s) = -\mathbb{1}_{\alpha=0} f(s) p_t(0, \mathrm{d}s) + \mathbb{1}_{\alpha=1} f(s) p_t(0, \mathrm{d}s) \\ - \mathbb{1}_{\alpha=1} g(s) p_t(1, \mathrm{d}s) + \mathbb{1}_{\alpha=0} g(s) p_t(1, \mathrm{d}s) \tag{2.8}$$

so that

$$\begin{cases} \partial_t p_t(0,s) + \dot{x}_c(t)\partial_s p_t(0,s) = & -f(s)p_t(0,s) + g(s)p_t(1,s), \\ \partial_t p_t(1,s) + \dot{x}_c(t)\partial_s p_t(1,s) = & -g(s)p_t(1,s) + f(s)p_t(0,s). \end{cases} \tag{2.9}$$

Let us now derive the equation on $P_\alpha(s,t)$ (defined in (2.4)). The s-marginal p_t^s evolution (2.3) is recovered from (2.2) integrating (2.9) over α. The time-evolution of the conditional law $P_\alpha(s,t)\mathrm{d}\alpha$ is then obtained from 2.5 and (2.9), giving

$$\begin{cases} \partial_t P_0(s,t) + \dot{x}_c(t)\partial_s P_0(s,t) = & -f(s)P_0(s,t) + g(s)P_1(s,t), \\ \partial_t P_1(s,t) + \dot{x}_c(t)\partial_s P_1(s,t) = & -g(s)P_1(s,t) + f(s)P_0(s,t), \end{cases}$$

which exactly recovers the previous system (1.1): a SDE representation has thus been built.

2.1. **Hill's thermodynamic formalism**

Assume an energy function $\overline{w}(\alpha,s) = \mathbb{1}_{\alpha=0}\overline{w}_0(s) + \mathbb{1}_{\alpha=1}\overline{w}_1(s)$ is associated to the system ($\overline{w}_\alpha$ is the energy related to the state α). The energy $\overline{w}_0$ characterizes the detached state, while $\overline{w}_1$ is the energy of an attached head. The use of a bar notation for the energies $\overline{w}_{0,1}$ will become clear in section 4.1.

Energy balance. The internal energy of the system at time t is the average

$$\mathcal{U}(t) := \mathbb{E}\left[\overline{w}(\alpha_t, s_t)\right] = \int_{\{0,1\}\times\mathbb{T}_d} \overline{w}(\alpha,s)\, p_t(\mathrm{d}\alpha, \mathrm{d}s).$$

The previous knowledge (2.4) on $p_t(\mathrm{d}\alpha, \mathrm{d}s)$ allows to write

$$\mathcal{U}(t) = \frac{1}{d}\int_{\mathbb{T}_d} \left[\overline{w}_0(s)P_0(s,t) + \overline{w}_1(s)P_1(s,t)\right]\mathrm{d}s$$

Moreover, the active force is defined as

$$\tau_c(t) := \mathbb{E}\left[\mathbb{1}_{\alpha_t=1}\partial_s\overline{w}(\alpha_t,s_t)\right] = \frac{1}{d}\int_{\mathbb{T}_d} \frac{\mathrm{d}\overline{w}_1(s)}{\mathrm{d}s} P_1(s,t)\mathrm{d}s$$

Using equation (1.1) to take the time-derivative of $\mathcal{U}(t)$:

$$\frac{\mathrm{d}}{\mathrm{d}t}\mathcal{U}(t) = \dot{\mathcal{W}}(t) - \frac{1}{d}\int_{\mathbb{T}_d} \left[\overline{w}_1(s) - \overline{w}_0(s)\right]\left[g(s)P_1(s,t) - f(s)P_0(s,t)\right]\mathrm{d}s$$

The first term

$$\dot{\mathcal{W}}(t) := \dot{x}_c(t)\tau_c(t) + \frac{\dot{x}_c(t)}{d}\int_{\mathbb{T}_d} \frac{\mathrm{d}\overline{w}_0(s)}{\mathrm{d}s} P_0(s,t)\mathrm{d}s$$

being the instantaneous power of external efforts. In sarcomere modelling, the detachment $1 \to 0$ at s_t is caused by an external energy input μ_T, which stands for ATP consumption: μ_T is a constant which embodies the necessary energy input for state change. For jumps to occur from higher energy states to lower energy ones, it is relevant to assume

$$\overline{w}_1(s) \le \overline{w}_0(s) \le \overline{w}_1(s) + \mu_T$$

so that attachment is a natural process which causes a decrease in state energy from $\overline{w}_0(s)$ to $\overline{w}_1(s)$, and then the external supply of μ_T allows going back to a state with energy $\overline{w}_0(s)$. Since ATP is buffered by the metabolic system, μ_T is a fixed parameter. The related flux term in the balance reads

$$\dot{\mathcal{E}}(t) := \frac{1}{d}\int_{\mathbb{T}_d} \mu_T\left[g(s)P_1(s,t) - f(s)P_0(s,t)\right]\mathrm{d}s.$$

The fluctuation around this flux of the energy transfer during the detachment is $\mathbb{1}_{\alpha_t=0}\overline{w}(\alpha_t,s_t) - \mathbb{1}_{\alpha_{t^-}=1}\overline{w}(\alpha_{t^-},s_{t^-}) - \mu_T$. In the balance, this thermal fluctuation stands for the heat dissipation

$$\dot{\mathcal{Q}}(t) := -\frac{1}{d}\int_{\mathbb{T}_d} \left[\overline{w}_1(s) + \mu_T - \overline{w}_0(s)\right]\left[g(s)P_1(s,t) - f(s)P_0(s,t)\right]\mathrm{d}s$$

so that the energetic balance corresponds to *the first principle of thermodynamics*

$$\frac{\mathrm{d}}{\mathrm{d}t}\mathcal{U}(t) = \dot{\mathcal{W}}(t) + \dot{\mathcal{E}}(t) + \dot{\mathcal{Q}}(t). \tag{2.10}$$

Remark 2.1. There's no energy left for thermal fluctuation in the case $\mu_T = \overline{w}_0(s) - \overline{w}_1(s)$ (in this case, no extra energy has to be dissipated as heat). The quantities τ_c and μ_T, together with this balance and the next one will be crucial to perform macroscopic coupling; an additional dependence of μ_T on t could be added. Note the term $J(s,t) = g(s)P_1(s,t) - f(s)P_0(s,t)$ corresponds to a probability flux which stands for the probability mass transfer $1 \to 0$.

Free energy balance. Let's compute the entropy balance. Following Hill's formalism [22, 24], the chemical potential of state α at time t is defined as

$$\mu_t(\alpha, s) := \overline{w}(\alpha, s) + k_B T \ln P_\alpha(s,t) = \mathbb{1}_{\alpha=0}\mu_t^0(s) + \mathbb{1}_{\alpha=1}\mu_t^1(s)$$

with the state chemical potentials at time t

$$\mu_t^0(s) = \overline{w}_0(s) + k_B T \ln P_0(s,t) \qquad \mu_t^1(s) = \overline{w}_1(s) + k_B T \ln P_1(s,t)$$

Free energy is then defined as

$$\mathcal{F}(t) := \mathbb{E}\left[\mu_t(\alpha_t, s_t)\right] = \frac{1}{d}\int_{\mathbb{T}_d} \left[\mu_t^0(s)P_0(s,t) + \mu_t^1(s)P_1(s,t)\right] \mathrm{d}s$$

The time-derivative of $\mathcal{F}(t)$ reads

$$\begin{aligned}\frac{\mathrm{d}}{\mathrm{d}t}\mathcal{F}(t) &= \frac{1}{d}\int_{\mathbb{T}_d} \partial_t P_0(s,t)\left[\overline{w}_0(s) + k_B T \ln\left(P_0(s,t)\right) + 1\right] \mathrm{d}s \\ &\quad + \frac{1}{d}\int_{\mathbb{T}_d} \partial_t P_1(s,t)\left[\overline{w}_1(s) + k_B T \ln\left(P_1(s,t)\right) + 1\right] \mathrm{d}s \\ &= \frac{1}{d}\int_{\mathbb{T}_d} \mu_t^0(s)\,\partial_t P_0(s,t)\,\mathrm{d}s + \frac{1}{d}\int_{\mathbb{T}_d} \mu_t^1(s)\,\partial_t P_1(s,t)\,\mathrm{d}s\end{aligned}$$

using the normalization condition (2.6) to simplify. Equation (1.1) now leads to

$$\frac{\mathrm{d}}{\mathrm{d}t}\mathcal{F}(t) = \dot{\mathcal{W}}(t) + \dot{\mathcal{E}}(t) - \frac{1}{d}\int_{\mathbb{T}_d} \left[\mu_t^1(s) + \mu_T - \mu_t^0(s)\right]\left[g(s)P_1(s,t) - f(s)P_0(s,t)\right] \mathrm{d}s$$

the last term of this balance should equal $-T(t)\dot{S}_{\mathrm{prod}}(t)$ in order the second principle of thermodynamics to hold. To assert this, it is necessary to check that $\dot{S}_{\mathrm{prod}}(t)$ remains non-negative. For the entropy balance to respect the second law of thermodynamics, appendix B shows that to every jump must be associated a reverse jump (possibly very rare) whose rate must satisfy the detailed balance condition (B.1), which involves energy of the system before and after the jump. In the current case, the detached state has energy $\overline{w}_0(s)$ before attachment and $\overline{w}_1(s)$ after. At the time of detachment, the energy rises to $\overline{w}_1(s) + \mu_T$ (thanks to the ATP consumption input μ_T) and then goes back to $\overline{w}_0(s)$. Thus, the total attachment rate $f(s)$ can't be directly compared to $g(s)$ in a detailed balance condition, because the arrival energy $\overline{w}_1(s)$ after attachment is not the same as the starting energy $\overline{w}_1(s) + \mu_T$ at detachment time. To see this, rates must be split back as

$$f(s) = k_+(s) + k_+^{\mathrm{rev}}(s) \qquad g(s) = k_-(s) + k_-^{\mathrm{rev}}(s)$$

and must satisfy the detailed balance conditions

$$k_+(s) = \exp\left[-\frac{\overline{w}_1(s) - \overline{w}_0(s)}{k_B T}\right] k_+^{\mathrm{rev}}(s)$$

$$k_-(s) = \exp\left[-\frac{\overline{w}_0(s) - \overline{w}_1(s) - \mu_T}{k_B T}\right] k_-^{\mathrm{rev}}(s)$$

If $\overline{w}_1(s) \le \overline{w}_0(s) \le \overline{w}_1(s) + \mu_T$ as expected, then one can see that thermodynamics favors the direct jumps $k_+(s)$ and $k_-(s)$ with respect to the reverse ones (their rates are all the bigger as the energy gaps are important). Finally,

$$\begin{aligned}\frac{\mathrm{d}}{\mathrm{d}t}\mathcal{F}(t) = \dot{\mathcal{W}}(t) + \dot{\mathcal{E}}(t) &- \frac{1}{d}\int_{\mathbb{T}_d} \left[\mu_t^1(s) - \mu_t^0(s)\right]\left[k_+^{\mathrm{rev}}(s)P_1(s,t) - k_+(s)P_0(s,t)\right] \mathrm{d}s \\ &- \frac{1}{d}\int_{\mathbb{T}_d} \left[\mu_t^1(s) + \mu_T - \mu_t^0(s)\right]\left[k_-(s)P_1(s,t) - k_-^{\mathrm{rev}}(s)P_0(s,t)\right] \mathrm{d}s\end{aligned}$$

both the last terms being now non-positive thanks to the detailed balance conditions. The second law is now respected, but the definition of $\dot{\mathcal{E}}(t)$ has to be adapted for the above equality to hold. It now reads

$$\dot{\mathcal{E}}(t) := \frac{1}{d}\int_{\mathbb{T}_d} \mu_T \left[k_-(s)P_1(s,t) - k_-^{\mathrm{rev}}(s)P_0(s,t)\right] \mathrm{d}s$$

The previous first law (2.10) still holds in this framework, but the definition of the heat transfer must be similarly adapted:

$$\dot{\mathcal{Q}}(t) := -\frac{1}{d}\int_{\mathbb{T}_d} \left[\overline{w}_1(s) + \mu_T - \overline{w}_0(s)\right] \left[k_-(s)P_1(s,t) - k_-^{\mathrm{rev}}(s)P_0(s,t)\right] \mathrm{d}s$$

leading to a fully consistent thermodynamic system.

3. The h-model

A Langevin like-model is built here such that the chosen site is the closest neighbor to the myosin head, and no more to the base point, see Fig. 2(b). The head is now introduced as an explicit variable X_t, which can move on the full real line: it is no more constrained within a torus, allowing desirable Lipschitz assumptions on rates. In the detached state, the dynamic of X_t tends to minimize a detached-state confinement potential w_0 (for instance a quadratic well, seeing the cross-bridge as a spring), but is still subjected to thermal fluctuations leading to an overdamped Langevin diffusion

$$\mathrm{d}X_t = -\eta^{-1}\nabla w_0(X_t)\mathrm{d}t + \sqrt{2k_BT/\eta}\ \mathrm{d}B_t,$$

the process $(B_t)_{t\geq 0}$ being a brownian motion (independent of the considered Poisson random measures), k_B the Boltzmann constant, T the temperature, and η a (high) damping coefficient. In case of a quadratic w_0, this corresponds to a noisy harmonic (Langevin) oscillator in the high-damping (or low-mass) limit (also known as Ornstein-Uhlenbeck process).

An additional variable is needed to keep track of the closest actin site to X_t. This latter site is always at most $d/2$ far from the moving head X_t, so an eulerian parametrization is well-adapted: let h_t be the algebraic distance in the torus $\mathbb{T}_d$ of X_t to its closest neighbor so that $s_t = X_t + \overline{h}_t$ (for a suitable projection $h \mapsto \overline{h}$ of the torus on $[-d/2, +d/2)$ or $(-d/2, +d/2]$). A moving (X_t-dependent) referential is used, and the X_t-dynamics shall impinge on the h_t-dynamics. Obviously h_t is useless when $\alpha_t = 1$ since then $h_t = 0$ (X_t then corresponds to the actin site location to which the head is attached). The couple (X_t, h_t) then appears as the natural structural variable.

A single jump site is allowed given X_t, which must be less than $d/2$ far: $d/2$ is no more the maximal extension for the cross-bridge, but it is the maximal allowed jump amplitude, i.e. the biggest instantaneous discontinuity which can be encountered for the position. This can be considered as a two-state multi-site model, because the myosin head is allowed to explore all the actin fiber, even if the jump amplitude remains bounded.

3.1. SDE formulation

The variable h_t lives in the torus $\mathbb{T}_d$: it is the algebraic distance from the myosin head X_t to the nearest actin site, whose position is

$$s_t := X_t + \overline{h}_t,$$

a representation $\overline{h}$ in $[-d/2, +d/2[$ or in $]-d/2, +d/2]$ being chosen for a variable h in $\mathbb{T}_d$. This latter choice shall not affect the dynamics, as long as attachment rates $k_+(x,h)$ and $k_-^{\mathrm{rev}}(x,h)$ vanish when h reaches the "boundary point". The dynamics can be seen as a Markov process

$$(X_t, \alpha_t, h_t) \in \mathbb{R} \times \{0,1\} \times \mathbb{T}_d,$$

the state variable α_t indicating whether the head is attached or not. The SDE system for this relative coordinate model reads

$$
\begin{cases}
\mathrm{d}X_t &= \left[\alpha_t \dot{x}_c(t) - (1-\alpha_t)\,\eta^{-1}\partial_x w_{\alpha_t}(X_t)\right]\mathrm{d}t + (1-\alpha_t)\sqrt{\frac{2k_BT}{\eta}}\mathrm{d}B_t \\
&\quad + (1-\alpha_{t^-})\int_{\mathbb{R}_+} \overline{h}_{t^-}\mathbb{1}_{u\le k_+\left(X_{t^-},h_{t^-}\right)}N_+(\mathrm{d}t,\mathrm{d}u) \\
&\quad + \alpha_{t^-}\int_{\mathbb{T}_d\times\mathbb{R}_+} -\overline{h}\mathbb{1}_{u\le \overline{k}_+^{\mathrm{rev}}\left(X_{t^-},h'\right)}N_+^{\mathrm{rev}}(\mathrm{d}t,\mathrm{d}h',\mathrm{d}u) \\
&\quad + \alpha_{t^-}\int_{\mathbb{T}_d\times\mathbb{R}_+} -\overline{h}\mathbb{1}_{u\le \overline{k}_-\left(X_{t^-},h'\right)}N_-(\mathrm{d}t,\mathrm{d}h',\mathrm{d}u) \\
&\quad + (1-\alpha_{t^-})\int_{\mathbb{R}_+} \overline{h}_{t^-}\mathbb{1}_{u\le k_-^{\mathrm{rev}}\left(X_{t^-},h_{t^-}\right)}N_-^{\mathrm{rev}}(\mathrm{d}t,\mathrm{d}u) \\
\mathrm{d}\alpha_t &= (1-\alpha_{t^-})\int_{\mathbb{R}_+}(1-2\alpha_{t^-})\,\mathbb{1}_{u\le k_+\left(X_{t^-},h_{t^-}\right)}N_+(\mathrm{d}t,\mathrm{d}u) \\
&\quad + \alpha_{t^-}\int_{\mathbb{T}_d\times\mathbb{R}_+}(1-2\alpha_{t-})\,\mathbb{1}_{u\le \overline{k}_+^{\mathrm{rev}}\left(X_{t^-},h'\right)}N_+^{\mathrm{rev}}(\mathrm{d}t,\mathrm{d}h',\mathrm{d}u) \\
&\quad + \alpha_{t^-}\int_{\mathbb{T}_d\times\mathbb{R}_+}(1-2\alpha_{t-})\,\mathbb{1}_{u\le \overline{k}_-\left(X_{t^-},h'\right)}N_-(\mathrm{d}t,\mathrm{d}h',\mathrm{d}u) \\
&\quad + (1-\alpha_{t^-})\int_{\mathbb{R}_+}(1-2\alpha_{t-})\,\mathbb{1}_{u\le k_-^{\mathrm{rev}}\left(X_{t^-},h_{t^-}\right)}N_-^{\mathrm{rev}}(\mathrm{d}t,\mathrm{d}u) \\
\mathrm{d}h_t &= \dot{x}_c(t)\mathrm{d}t - \mathrm{d}X_t \qquad \text{in } \mathbb{T}_d
\end{cases}
\tag{3.1}
$$

As previously, four jumps have been introduced, see Fig. 3 provided they satisfy some detailed balance condition (3.4), these jumps will be responsible for the thermodynamics consistency of the model, as detailed in the next sections. These jumps are associated as previously to four independent random measures:

- N_+ and N_-^{rev} are Poisson random measures on $\mathbb{R}_+\times\mathbb{R}_+$ with intensity $\mathrm{d}t\otimes\mathrm{d}u$. They account for the jumps $0\to 1$, where X_t jumps to $X_t+\overline{h}_{t^-}$ (the integrand within the Poisson integral is indeed the jump amplitude).

- N_- and N_+^{rev} are Poisson random measures on $\mathbb{R}_+\times\mathbb{T}_d^0\times\mathbb{R}_+$ with intensity $\mathrm{d}t\otimes\mathrm{d}h\otimes\mathrm{d}u$. They account for the jumps $1\to 0$, where a new value is chosen at random for h_t (the law of this choice being specified by the kernels $\overline{k}_+^{\mathrm{rev}}$ and $\overline{k}_-$, following the procedure detailed in appendix A) and X_t jumps to X_t-h_t. The assumed link between rates k_+, $\overline{k}_-^{\mathrm{rev}}$ and k_+^{rev}, $\overline{k}_-$ is a detailed balance condition, which will be specified in the next sections.

Since no explosion has to be imposed on rates, well-posedness is directly obtained for this jump diffusion process, as an application of [18, Theorem 2.1]. The only condition is that the rates have to be bounded and Lipschitz on the torus. The Lipschitz condition can be verified on $[-d/2,d/2]$ and extended to the torus, provided $\varepsilon>0$ exists such that $k_+(x,h)$ and $k_-^{\mathrm{rev}}(x,h)$ vanish for $\overline{h}$ outside of $[-d/2+\varepsilon,d/2-\varepsilon]$.

Remark 3.1 (Role of rates and kernels). Notice that the rates k^+ and k_-^{rev} behave quite differently from the kernel $\overline{k}_-$ and $\overline{k}_+^{\mathrm{rev}}$. Indeed, k^+ and k_-^{rev} are jump rates for jumps $0\to 1$ in α_t (they quantify the frequency of these jump events), while $\overline{k}_-$ and $\overline{k}_+^{\mathrm{rev}}$ are kernels for the jump $1\to 0$, following the mechanism detailed in remark A.2 of appendix A.2: these kernels both contain the corresponding jump rates

$$
k_-(x) := \int_{\mathbb{T}_d}\overline{k}_-(x,h)\,\mathrm{d}h \qquad k_+^{\mathrm{rev}}(x) := \int_{\mathbb{T}_d}\overline{k}_+^{\mathrm{rev}}(x,h)\,\mathrm{d}h\,,
$$

together with the corresponding jump measures $K_-(x,\mathrm{d}h)$ and $K_+^{\mathrm{rev}}(x,\mathrm{d}h)$ such that

$$
\overline{k}_-\left(x,h'\right)\mathrm{d}h' = k_-(x)K_-(x,\mathrm{d}h') \qquad \overline{k}_+^{\mathrm{rev}}\left(x,h'\right)\mathrm{d}h' = k_+^{\mathrm{rev}}(x)K_+^{\mathrm{rev}}(x,\mathrm{d}h')\,.
$$

3.2. **PDE related system**

As in section 2, it is now possible to derive a system of PDE for the joint law $p_t(\mathrm{d}x,\mathrm{d}\alpha,\mathrm{d}h)$ of (X_t,α_t,h_t) at time t. This relies on computing the adjoint of the infinitesimal generator of the Markov process $((X_t,\alpha_t,h_t))_{t\ge 0}$. This generator sums the generators associated to each term of the SDE, the X_t-diffusion leading to a parabolic term of the kind

$$
-\eta^{-1}\partial_x w_0.\nabla + \frac{k_BT}{\eta}\Delta \tag{3.2}
$$

In the current case of a jump diffusion process, the generator is made explicit in appendix A. Assume that p_t has a density with respect to the Lebesgue measures on $\mathbb{R}_+$ and the torus, so that

$$p_t(\mathrm{d}x, 0, \mathrm{d}h) = p_t(x, 0, h)\mathrm{d}x\mathrm{d}h$$
$$p_t(\mathrm{d}x, 1, \mathrm{d}h) = p_t(x, 1)\mathrm{d}x\delta_0(\mathrm{d}h)$$

The second line involves a Dirac measure because $h_t = 0$ as soon as $\alpha_t = 1$. The Fokker-Planck system on p_t eventually reads (note that existence of a density is not required to give a weak sense to the following system)

$$\begin{cases} \partial_t p_t(x,0,h) = & -\dot{x}_c(t)\partial_h p_t(x,0,h) - \frac{2k_BT}{\eta}\partial_x\partial_h p_t(x,0,h) \\ & -\partial_h\left[\eta^{-1}\partial_x w_0\left(x\right) p_t(x,0,h) - \frac{k_BT}{\eta}\partial_h p_t(x,0,h)\right] \\ & +\partial_x\left[\eta^{-1}\partial_x w_0\left(x\right) p_t(x,0,h) + \frac{k_BT}{\eta}\partial_x p_t(x,0,h)\right] \\ & -\left[k_+\left(x,h\right) + k_-^{\mathrm{rev}}(x,h)\right] p_t(x,0,h) \\ & +\left[\overline{k}_-(x+\overline{h},h) + \overline{k}_+^{\mathrm{rev}}(x+\overline{h},h)\right] p_t(x+\overline{h},1) \\ \partial_t p_t(x,1) = & -\dot{x}_c(t)\partial_x p_t(x,1) \\ & -p_t(x,1)\int_{\mathbb{T}_d}\left[\overline{k}_-(x,h') + \overline{k}_+^{\mathrm{rev}}(x,h')\right]\mathrm{d}h' \\ & +\int_{\mathbb{T}_d}\left[k_+\left(x-\overline{h},h\right) + k_-^{\mathrm{rev}}(x-\overline{h},h)\right] p_t\left(x-\overline{h},0,h\right)\mathrm{d}h \end{cases} \tag{3.3}$$

The second and the third line correspond to the diffusion operator (3.2), which stands for the diffusion which drives $\mathrm{d}X_t$, and $\mathrm{d}h_t$ as well through the SDE. The cross differential $-\frac{2k_BT}{\eta}\partial_x\partial_h p_t(x,0,h)$ comes from the fact the X_t and h_t are driven by the same brownian noise. Since the coefficients of this linear PDE are Lipschitz continuous and bounded, well-posedness stems from the classical references [36, 44] Integrating and summing both equations gives

$$\int_{\mathbb{R}\times\mathbb{T}_d}\partial_t p_t(x,0,h)\mathrm{d}x\mathrm{d}h + \int_{\mathbb{R}}\partial_t p_t(x,1)\mathrm{d}x = 0$$

which is the expression of mass conservation for the probability measure p_t.

3.3. **Thermodynamic balances**

Thermodynamic balances can now be obtained as in section 2.1. The considered densities $p_t(x,0,h)$ and $p_t(x,1)$ respectively quantify the probability for the system to be in the states $(x,0,h)$ and $(x,1)$ at time t. *They don't directly correspond to the Huxley densities* $P_0(s,t)$ and $P_1(s,t)$ which were quantifying the *conditional* probability of being in state 0 or 1 knowing s. The energy function of the system is now $w\left(x,\alpha,h\right) = \mathbb{1}_{\alpha=0}w_0(x) + \mathbb{1}_{\alpha=1}w_1(x)$ is associated to the system (w_α is the energy related to the state α).

Energy balance. As previously, the first principle of thermodynamics reads

$$\frac{\mathrm{d}}{\mathrm{d}t}\mathcal{U}(t) = \dot{\mathcal{W}}(t) + \dot{\mathcal{E}}(t) + \dot{\mathcal{Q}}(t)$$

where $\mathcal{U}(t)$ is the average (internal) energy of the system, the instantaneous power of external efforts being

$$\dot{\mathcal{W}}(t) = \dot{x}_c(t)\tau_c(t) := \dot{x}_c(t)\int_{\mathbb{R}}\partial_x w_1(x)p_t(x,1)\mathrm{d}x$$

The ATP flux supplied by the external medium is

$$\dot{\mathcal{E}}(t) := \int_{\mathbb{R}\times\mathbb{T}_d}\left[\mu_T\overline{k}_-(x,h)p_t(x,1) - k_-^{\mathrm{rev}}(x,h)p_t(x,0,h)\right]\mathrm{d}x\mathrm{d}h$$

and the exchanged heat now reads

$$\begin{aligned}\dot{\mathcal{Q}}(t) = &- \int_{\mathbb{R}\times\mathbb{T}_d} \left(\partial_x w_0(x)\right)^2 p_t\left(x,0,h\right) \mathrm{d}x\mathrm{d}h + \frac{k_B T}{\eta} \int_{\mathbb{R}\times\mathbb{T}_d} \partial^2_{xx} w_0(x) p_t\left(x,0,h\right) \mathrm{d}x\mathrm{d}h \\ &+ \int_{\mathbb{R}\times\mathbb{T}_d} \left[w_0(x) - w_1(x)\right] \left[\overline{k}_+^{\mathrm{rev}}(x,h) p_t(x,1) - k_+(x,h) p_t\left(x,0,h\right)\right] \mathrm{d}x\mathrm{d}h \\ &+ \int_{\mathbb{R}\times\mathbb{T}_d} \left[w_1(x) + \mu_T - w_0(x)\right] \left[k_-^{\mathrm{rev}}(x,h) p_t\left(x,0,h\right) - \overline{k}_-(x,h) p_t\left(x,1\right)\right] \mathrm{d}x\mathrm{d}h\end{aligned}$$

Compared to the model in section 2.1, two new terms involving w_0 have appeared in the exchanged heat, due to the Langevin dynamics on x.

Free energy balance. The chemical state chemical potentials at time t are now

$$\mu_t^0\left(x,h\right) = w_0\left(x\right) + k_B T \ln p_t\left(x,0,h\right) \qquad \mu_t^1\left(x\right) = w_1\left(s\right) + k_B T \ln p_t\left(x,1\right)$$

Free energy is then as

$$\mathcal{F}(t) = \int_{\mathbb{R}\times\mathbb{T}_d} \mu_t^0(x) p_t\left(x,0,h\right) \mathrm{d}x\mathrm{d}h + \int_{\mathbb{R}} \mu_t^1(x) p_t\left(x,1\right) \mathrm{d}x$$

As previously, using mass conservation

$$\begin{aligned}\frac{\mathrm{d}}{\mathrm{d}t}\mathcal{F}(t) &= \int_{\mathbb{R}\times\mathbb{T}_d} \mu_t^0(x) \partial_t p_t\left(x,0,h\right) \mathrm{d}x\mathrm{d}h + \int_{\mathbb{R}} \mu_t^1(x) \partial_t p_t\left(x,1\right) \mathrm{d}x \\ &= \dot{\mathcal{W}}(t) + \dot{\mathcal{E}}(t) - T\dot{S}_{\mathrm{prod}}(t)\end{aligned}$$

where straightforward computations give

$$\begin{aligned}T\dot{S}_{\mathrm{prod}}(t) =& \eta^{-1} \int_{\mathbb{R}\times\mathbb{T}_d} \left(\partial_x \mu_t^0(x,h) - \partial_h \mu_t^0(x)\right)^2 p_t\left(x,0,h\right) \mathrm{d}x\mathrm{d}h \\ &+ \int_{\mathbb{R}\times\mathbb{T}_d} \left[\mu_t^0(x,h) - \mu_t^1(x+\overline{h})\right] \left[k_+(x,h) p_t\left(x,0,h\right) - \overline{k}_+^{\mathrm{rev}}(x+\overline{h},h) p_t\left(x+\overline{h},y,1\right)\right] \mathrm{d}x\mathrm{d}h \\ &+ \int_{\mathbb{R}\times\mathbb{T}_d} \left[\mu_t^1(x) + \mu_T - \mu_t^0(x-\overline{h},h)\right] \left[\overline{k}_-(x,h) p_t\left(x,1\right) - k_-^{\mathrm{rev}}(x-\overline{h},h) p_t\left(x-\overline{h},0,h\right)\right] \mathrm{d}x\mathrm{d}h\end{aligned}$$

In order the second law of thermodynamics to hold, it is necessary to check that $\dot{S}_{\mathrm{prod}}(t)$ remains non-negative. Following appendix B, this will be true provided the following detailed balance conditions hold:

$$k_+^{\mathrm{rev}}(x) K_+^{\mathrm{rev}}\left(x,\mathrm{d}h'\right) = \exp\left[-\frac{w_0(x-\overline{h'}) - w_1(x)}{k_B T}\right] k_+\left(x-\overline{h'},h'\right) \mathrm{d}h' \tag{3.4}$$

$$k_-\left(x\right) K_-\left(x,\mathrm{d}h'\right) = \exp\left[-\frac{w_0(x-\overline{h'}) - w_1(x) - \mu_T}{k_B T}\right] k_-^{\mathrm{rev}}(x-\overline{h'},h')\mathrm{d}h \tag{3.5}$$

Starting from the attached configuration, the detachment must choose the new h_t after the jump (the new position is then $X_t - h_t$). The law $K_-\left(x,\mathrm{d}h\right)$ is imposed by the above detailed balance condition. The same holds for the reverse attachment jump and the law $K_+^{\mathrm{rev}}\left(x,\mathrm{d}h\right)$. These jump measures being normalized, this imposes

$$k_+^{\mathrm{rev}}(x) = \int_{\mathbb{T}_d} \exp\left[-\frac{w_0(x-\overline{h}) - w_1(x)}{k_B T}\right] k_+\left(x-\overline{h},h\right) \mathrm{d}h \tag{3.6}$$

$$k_-\left(x\right) = \int_{\mathbb{T}_d} \exp\left[-\frac{w_0(x-\overline{h}) - w_1(x) - \mu_T}{k_B T}\right] k_-^{\mathrm{rev}}(x-\overline{h},h)\mathrm{d}h \tag{3.7}$$

It is thus sufficient to know the rates $k_+\left(x,h\right)$ and $k_-^{\mathrm{rev}}(x,h)$ to determine all the jump features.

4. **Model reduction**

The next section is concerned with model reduction. The first part verifies that this relative coordinate model recovers back the Huxley model when assuming the head stays in the fixed window $\mathbb{T}_d$. The second part proposes an extension of the Huxley model to the whole real line: the assumption of restricted window can be removed, up to adding some correction term.

4.1. **Recovering the Huxley model back**

The previous model is expected to recover in the Huxley system (2.9) in some suitable limit: to do so, it must be assumed that X_t stays within the torus $\mathbb{T}_d$. In particular $\overline{h}$ is no more needed: h can be directly considered, since everything now lives in $\mathbb{T}_d$. It is easy to introduce back the closet site s in $\mathbb{T}_d$, considering the change of variable $s = x + h$ and

$$\overline{p}_t(x, \alpha, s) = p_t(x, \alpha, s - x) \qquad \text{for } s \text{ in } \mathbb{T}_d\,.$$

This leads

$$\begin{aligned}\partial_x \overline{p}_t(x, \alpha, s) &= \partial_x p_t(x, \alpha, s - x) - \partial_h p_t(x, \alpha, s - x)\\ \partial^2_{xx} \overline{p}_t(x, \alpha, s) &= \partial^2_{xx} p_t(x, \alpha, s - x) - 2\partial_x \partial_h p_t(x, \alpha, s - x) + \partial^2_{hh} p_t(x, \alpha, s - x)\,,\end{aligned}$$

and so on for the crossed-derivatives. Rewriting the system as

$$\begin{cases}\partial_t \overline{p}_t(x, 0, s) = & -\dot{x}_c(t)\partial_s \overline{p}_t(x, 0, s)\\ & +\partial_x \left[\eta^{-1}\partial_x w_0\,(x)\,\overline{p}_t(x, 0, s) + \frac{k_B T}{\eta}\partial_x \overline{p}_t(x, 0, s)\right]\\ & -\left[k_+\,(x, s - x) + k^{\mathrm{rev}}_-(x, s - x)\right]\overline{p}_t(x, 0, s)\\ & +\left[\overline{k}_-(s, s - x) + \overline{k}^{\mathrm{rev}}_+(s, s - x)\right] p_t(s, 1)\\ \partial_t p_t(s, 1) = & -\dot{x}_c(t)\partial_s p_t(s, 1)\\ & -p_t(s, 1)\int_{\mathbb{T}_d}\left[\overline{k}_-(s - h', h') + \overline{k}^{\mathrm{rev}}_+(s - h', h')\right]\mathrm{d}h\\ & +\int_{\mathbb{T}_d}\left[k_+\left(x - \overline{h}, h\right) + k^{\mathrm{rev}}_-(s - \overline{h}, h)\right]\overline{p}_t\left(s - \overline{h}, 0, h\right)\mathrm{d}h\end{cases}$$

Following [7], there are two possible ways to recover from this a closed system like (2.9), which *only depend on* s:

- *Adiabatic elimination*: this approach considers x to be at thermal equilibrium independently of s, assuming
$$\overline{p}_t(x, 0, s) = \overline{p}^{\mathrm{th}}_0\,(x)\,p_t(s, 0)$$
defining the equilibrium probability density $\overline{p}^{\mathrm{th}}_0\,(x) := Z^{-1}\exp\left[-\frac{w_0(x)}{k_B T}\right]$, Z being the adequate normalization constant. This suggests to consider the s-dependent rates
$$\begin{aligned}f(s) &:= \int_{\mathbb{T}_d}\left[k_-(s, s - x) + k^{\mathrm{rev}}_+(s, s - x)\right]\overline{p}^{\mathrm{th}}_0\,(x)\,\mathrm{d}x\\ g(s) &:= \int_{\mathbb{T}_d}\left[\overline{k}_-(s - h, h') + \overline{k}^{\mathrm{rev}}_+(s - h', h')\right]\mathrm{d}h\,.\end{aligned}$$
Integrating the above PDE system over s then exactly recovers (2.9).

- *Direct elimination*: let's set
$$\begin{aligned}f(s) &:= \overline{k}_-(s, s - x) + \overline{k}^{\mathrm{rev}}_+(s, s - x)\\ g(s) &:= \int_{\mathbb{T}_d}\left[k_-(s - h, h) + k^{\mathrm{rev}}_+(s - h, h)\right]\mathrm{d}h\,,\end{aligned}$$
assuming that $k_-(s, s - x) + k^{\mathrm{rev}}_+(s, s - x)$ *only depends on* s. Considering now
$$p_t(s, 0) := \int_{\mathbb{T}_d}\overline{p}_t(x, 0, s)\mathrm{d}x$$
and integrating the PDE system over s then recovers (2.9) too.

Note however that this limit imposes to face the difficulties explained in the introduction, because X_t has to be constrained to stay within $\mathbb{T}_d$.

4.2. **A reduced model which generalizes the Huxley one**

The current model allows more general (and physiologically relevant) displacements, since X_t can now move on the whole real line. The counterpart is the need for two variables X_t, h_t in order to describe the $\alpha_t = 0$ dynamics: the convenient shortcut s_t is not directly available, since its domain is now x-dependent. Nonetheless, some simplifications are still possible, allowing to derive an analog of the Huxley model (parameterized by s_t only) which would stay valid on the whole real line. Introducing the Huxley parameter $s = x + \overline{h}$ and the related densities

$$p_t^0(s,h) := p_t(s-\overline{h},0,h) \qquad \overline{p}_t^1(s) := p_t^1(s,1)$$

For $-d/2 < \overline{h} < +d/2$, this change of variable leads to

$$\partial_h p_t^0(s,h) = -\partial_x p_t(s-\overline{h},0,h) + \partial_h p_t(s-\overline{h},0,h)\,,$$

and other derivatives can be computed in the same way, to rewrite the system as

$$\begin{cases} \partial_t p_t^0(s,h) = & -\dot{x}_c(t)\partial_h p_t^0(s,h) - \dot{x}_c(t)\partial_s p_t^0(s,h) \\ & -\partial_h\left[\eta^{-1}\partial_x w_0\left(s-\overline{h}\right)p_t^0(s,h) - \frac{k_BT}{\eta}\partial_h p_t^0(s,h)\right] \\ & -\left[k_+\left(s-\overline{h},h\right) + k_-^{\mathrm{rev}}(s-\overline{h},h)\right]p_t^0(s,h) \\ & +\left[\overline{k}_-(s,h) + \overline{k}_+^{\mathrm{rev}}(s,h)\right]\overline{p}_t^1(s) \\ \partial_t \overline{p}_t^1(s) = & -\dot{x}_c(t)\partial_x \overline{p}_t^1(s) \\ & -\overline{p}_t^1(s)\int_{\mathbb{T}_d}\left[\overline{k}_-(s,h') + \overline{k}_+^{\mathrm{rev}}(s,h')\right]\mathrm{d}h' \\ & +\int_{\mathbb{T}_d}\left[k_+(s-h,h) + k_-^{\mathrm{rev}}(s-h,h)\right]p_t^0(s,h)\mathrm{d}h \end{cases}$$

The density p_t^0 *can now be searched as a continuous function on* $\mathbb{R}\times(-d/2,d/2)$ that solves the above PDE system adding a "periodic boundary condition"

$$\lim_{\substack{h\to -d/2\\ h>-d/2}} p_t^0(s,h) = \lim_{\substack{h\to +d/2\\ h<+d/2}} p_t^0(s+d,h)$$

By continuity, $p_t^0(s,h)$ and its derivatives can then be extended to $h = \pm d/2$ such that

$$p_t^0(s,-d/2) = p_t^0(s+d,d/2). \tag{4.1}$$

This extension accounts for the situation where the actin head x is equally far from two actin sites: since $x = s-h$ having $(s,-d/2)$ or $(s+d,d/2)$ corresponds to the same situation and the same value of x. Integrating over h the equation on $p_t^0(s)$ now gives the exact relation

$$\begin{aligned} \int_{\mathbb{T}_d}\partial_t p_t^0(s,h)\mathrm{d}h = & -\dot{x}_c(t)\left[p_t^0(s,d/2) - p_t^0(s,-d/2)\right] - \dot{x}_c(t)\partial_s\overline{p}_t^0(s) \\ & -\eta^{-1}\left[\partial_x w_0\left(s-d/2\right)p_t^0(s,d/2) - \partial_x w_0\left(s+d/2\right)p_t^0(s,-d/2)\right] \\ & +\tfrac{k_BT}{\eta}\left[\partial_h p_t^0(s,d/2) - \partial_h p_t^0(s,-d/2)\right] \\ & -\int_{\mathbb{T}_d}\left[k_+(s-\overline{h},h) + k_-^{\mathrm{rev}}(s-\overline{h},h)\right]p_t^0(s,h)\mathrm{d}h \\ & +\overline{p}_t^1(s)\int_{\mathbb{T}_d}\left[\overline{k}_-(s,h) + \overline{k}_+^{\mathrm{rev}}(s,h')\right]\mathrm{d}h' \end{aligned} \tag{4.2}$$

and thanks to the periodicity relation (4.1), the first three lines become:

$$\begin{aligned} & -\dot{x}_c(t)\left[p_t^0(s,d/2) - p_t^0(s+d,d/2)\right] - \dot{x}_c(t)\partial_s\overline{p}_t^0(s) \\ & -\eta^{-1}\left[\partial_x w_0\left(s-d/2\right)p_t^0(s,d/2) - \partial_x w_0\left(s+d/2\right)p_t^0(s+d,d/2)\right] \\ & +\tfrac{k_BT}{\eta}\left[\partial_h p_t^0(s,d/2) - \partial_h p_t^0(s+d,d/2)\right] \end{aligned} \tag{4.3}$$

As in section 4.1, a possible way to recover a closed system in the only variable s is now the adiabatic elimination of h given s, *assuming* that

$$p_t^0(s,h) = \overline{p}_t^0(s)p_0^{\mathrm{th}}(h|s) \qquad p_0^{\mathrm{th}}(h|s) = \frac{1}{Z_0(s)}\exp\left[-\frac{w_0\left(s-h\right)}{k_BT}\right], \tag{4.4}$$

where the thermalized density p_0^{th} stands for the conditional law of h given s, whose partition function is defined as

$$Z_0(s) := \int_{-d/2}^{d/2}\exp\left[-\frac{w_0(s-h)}{k_BT}\right]\mathrm{d}h\,. \tag{4.5}$$

Note that since this *closure assumption* is only an approximation, the periodicity relation (4.1) *won't be verified anymore*. Our h-reduced model results from this approximation, which mimics the dynamics $(t,s) \mapsto \overline{p}_t^0(s), \overline{p}_t^1(s)$. We define moreover

$$f(s) := \int_{\mathbb{T}_d} \left[k_+(s-\overline{h},h) + k_-^{\mathrm{rev}}(s-\overline{h},h)\right] p_0^{\mathrm{th}}(h|s)\mathrm{d}h \qquad g(s) := \int_{\mathbb{T}_d} \left[\overline{k}_-(s,h') + \overline{k}_+^{\mathrm{rev}}(s,h')\right] \mathrm{d}h' \,. \tag{4.6}$$

Considering h to be at thermal equilibrium allows to cancel the diffusion terms in (4.2), leading to the following system:

$$\begin{cases} \partial_t \overline{p}_t^0(s) = & -\dot{x}_c(t)\left[p_0^{\mathrm{th}}(d/2|s)\overline{p}_t^0(s) - p_0^{\mathrm{th}}(d/2|s+d)\overline{p}_t^0(s+d)\right] - \dot{x}_c(t)\partial_s \overline{p}_t^0(s) \\ & -f(s)\overline{p}_t^0(s) + g(s)\overline{p}_t^1(s) \\ \partial_t \overline{p}_t^1(s) = & -\dot{x}_c(t)\partial_s \overline{p}_t^1(s) - g(s)\overline{p}_t^1(s) + f(s)\overline{p}_t^0(s), \end{cases} \tag{4.7}$$

which is the desired generalization of the Huxley system (2.9) to the full real line.

Remark 4.1 (An alternative direct elimination). Keeping the same $g(s)$, an alternative elimination analogous to section 4.1 would have been to directly assume that

$$f(s) := k_+(s,h) + k_-^{\mathrm{rev}}(s,h)$$

no more depends on h. Define then the marginal distribution

$$\overline{p}_t^0(s) := \int_{\mathbb{T}_d} p_t^0(s,h)\mathrm{d}h \,,$$

whose time-evolution is given by (4.2). To turn (4.2) into a closed equation on $\overline{p}_t^0(s)$, values have to be postulated for $p_t^0(s,d/2)$ and $\partial_h p_t^0(s,d/2)$. Since $p_t^0(s,d/2)$ and $\partial_h p_t^0(s,d/2)$ are going to be replaced by plausible approximate values, the periodicity relation (4.1) won't be (exactly) verified anymore. A natural choice here (but others would be possible too) would be at $h = \pm d/2$ to use the values given by the adiabatic elimination (4.4), giving the same system as (4.7), but with a slightly different coefficient $g(s)$. Assuming as above, that the whole h-density is thermalized, seems more consistent though.

Remark 4.2 (Interpretation of the correction term). The terms, which involve $p_t^0(s,d/2) = p_0^{\mathrm{th}}(d/2|s)\,\overline{p}_t^0(s)$, are reminiscent of the periodicity relation (4.1) and the fact a myosin head doesn't discriminate sites which are equally far from it. If a site located at s translates with positive speed $\dot{x}_c(t) > 0$ (to fix ideas), it is no longer the closest site to myosin heads which were located at $x = s - d/2$, hence the loss of the related probability mass and the term $-\dot{x}_c(t)p_t^0(s,d/2)$. In the same way, the actin site located at $s+d$ translates and is no more the closest site to myosin heads located at $x = s + d/2$: for such a site, the closest becomes the one which was in s, hence a gain of probability mass and the term $+\dot{x}_c(t)p_t^0(s+d,d/2)$.

Remark 4.3 (Loss of the periodicity relation). As explained above, the periodicity relation (4.1) is now lost, because the obtained system is only an approximation of the exact marginal dynamics (4.2). If this relation were true, this would read for the closure choice (4.4):

$$Z_0^{-1}(s)\overline{p}_t^0(s) = Z_0^{-1}(s+d)\overline{p}_t^0(s+d) \tag{4.8}$$

The fact *this relation is not true* will later give insights on the thermodynamic balances.

Remark 4.4 (A jump interpretation for the correction term). As explained in remark 4.2, the correction term

$$-\dot{x}_c(t)\left[p_0^{\mathrm{th}}(d/2|s)\overline{p}_t^0(s) - p_0^{\mathrm{th}}(d/2|s+d)\overline{p}_t^0(s+d)\right]$$

appearing in (4.7) stands for the fact that if a site s translates with positive speed $\dot{x}_c(t) > 0$, it will no longer be the closest site to myosin heads located at $x = s - d/2$ (but $s-d$ becomes this site), hence a loss of a probability mass to the site located at $s-d$ (and a gain from the one at $s+d$). To subtract the right probability mass, one needs to know the probability for a myosin head to be at $x = s - d/2$, i.e. the probability for h to equal $d/2$ given an actin site in s. With the choice (4.4), this quantity is precisely $p_0^{\mathrm{th}}(d/2|s)$, hence the related weight.

If the energy function w_0 is convex, one can check that $s \mapsto p_0^{\mathrm{th}}(d/2|s)$ decreases provided s is large enough: this is reminiscent of the X_t-dynamics. Indeed, the variable s on the real line is not allowed to escape too far from the origin, since it is the location of *the closest site to the myosin head*, and no more a given reference actin site. Although the X_t variable has been eliminated, the myosin head X_t was evolving in the confinement potential w_0, and this feature is recovered there in the resulting s-dynamics. This will also appear in the detailed balance conditions for (4.7).
Finally, since the correction term only corresponds to a mass transfer of s to $s-d$, it is possible to write a SDE interpretation of this system, using a new Poisson random measure $N_{\mathrm{corr}}(\mathrm{d}t, \mathrm{d}u)$ on $\mathbb{R}_+ \times \mathbb{R}_+$ with intensity $\mathrm{d}t \otimes \mathrm{d}u$ (independent of the other ones):

$$\begin{cases} \mathrm{d}\alpha_t = & (1-\alpha_{t^-}) \int_{\mathbb{R}_+} (1-2\alpha_{t^-})\, \mathbb{1}_{u \le f(s_{t^-})} N_+(\mathrm{d}t, \mathrm{d}u) \\ & +\alpha_{t^-} \int_{\mathbb{R}_+} (1-2\alpha_{t^-})\, \mathbb{1}_{u \le g(s_{t^-})} N_-(\mathrm{d}t, \mathrm{d}u) \\ \mathrm{d}s_t = & \dot{x}_c(t)\mathrm{d}t - (1-\alpha_{t^-}) \int_{\mathbb{R}_+} d\mathbb{1}_{u \le \dot{x}_c(t) p_0^{\mathrm{th}}(d/2|s_{t^-})} N_{\mathrm{corr}}(\mathrm{d}t, \mathrm{d}u) \qquad \text{in } \mathbb{R} \end{cases} \tag{4.9}$$

This additional jump on s_t stands from this probability mass transfer as long as s_t translates with speed $\dot{x}_c(t) > 0$. This provides *a SDE representation for the Huxley-like system* (4.7).

Remark 4.5 (Case of a negative speed). Assume now that $\dot{x}_c(t) < 0$. The PDE system (4.7) still makes sense, but the related SDE interpretation (4.9) no longer holds because the jump rate $\dot{x}_c(t) p_0^{\mathrm{th}}(d/2|s_{t^-})$ of the Poisson clock is no longer positive. If one wants to keep this interpretation (which is useful for numerical simulations), it is possible to write an alternative version of the model in this case. Going back to (4.2) and using the periodicity relation (4.1), one can write alternatively to (4.3):

$$\begin{array}{l} -\dot{x}_c(t) \left[p_t^0(s-d, -d/2) - p_t^0(s, -d/2) \right] - \dot{x}_c(t) \partial_s \overline{p}_t^0(s) \\ -\eta^{-1} \left[\partial_x w_0\left(s - d/2\right) p_t^0(s-d, -d/2) - \partial_x w_0\left(s + d/2\right) p_t^0(s, -d/2) \right] \\ +\frac{k_B T}{\eta} \left[\partial_h p_t^0(s-d, -d/2) - \partial_h p_t^0(s, -d/2) \right] \end{array}$$

Applying now the same closure choice (4.4), this suggests an alternative to (4.7) where the correction term has been replaced by

$$-\dot{x}_c(t) p_0^{\mathrm{th}}(-d/2|s-d) \overline{p}_t^0(s-d) + \dot{x}_c(t) p_0^{\mathrm{th}}(-d/2|s) \overline{p}_t^0(s)$$

Since the coefficient $\dot{x}_c(t) p_0^{\mathrm{th}}(-d/2|s)$ is now negative, this admits the SDE representation

$$\begin{cases} \mathrm{d}\alpha_t = & (1-\alpha_{t^-}) \int_{\mathbb{R}_+} (1-2\alpha_{t^-})\, \mathbb{1}_{u \le f(s_{t^-})} N_+(\mathrm{d}t, \mathrm{d}u) \\ & +\alpha_{t^-} \int_{\mathbb{R}_+} (1-2\alpha_{t^-})\, \mathbb{1}_{u \le g(s_{t^-})} N_-(\mathrm{d}t, \mathrm{d}u) \\ \mathrm{d}s_t = & \dot{x}_c(t)\mathrm{d}t + (1-\alpha_{t^-}) \int_{\mathbb{R}_+} d\mathbb{1}_{u \le -\dot{x}_c(t) p_0^{\mathrm{th}}(-d/2|s_{t^-})} N_{\mathrm{corr}}(\mathrm{d}t, \mathrm{d}u) \qquad \text{in } \mathbb{R} \end{cases}$$

The correction jump $s \to s-d$ has thus been replaced by a jump $s \to s+d$. Note that this approach would be equivalent to the previous one if the periodicity relation (4.8) were true for the approximated model (4.7).

Remark 4.6 (Conditional Huxley-like densities). The densities $\overline{p}_t^0$ and $\overline{p}_t^1$ respectively quantify the probability for the system to be in state $(0, s)$ and $(1, s)$: those aren't the conditional densities $P_0(s,t)$ and $P_1(s,t)$ of being in states 0 and 1 when already knowing s. Since the marginal law $p_t^s = \overline{p}_t^0 + \overline{p}_t^1$ of s can't be determined alone anymore (see (4.10) in the next section), these latter conditional densities, defined by

$$P_0(s,t) := \frac{\overline{p}_t^0(s)}{p_t^s(s)} \qquad P_1(s,t) := \frac{\overline{p}_t^1(s)}{p_t^s(s)}$$

become of second interest. It is not directly possible to write an evolution PDE for them (but it would be possible if the periodicity relation (4.8) was true). However, they can still be computed from the above relations, after computing $\overline{p}_t^0$ and $\overline{p}_t^1$.

4.3. **Reduced thermodynamic balance**

Let us now establish the physical and chemical properties of the reduced model (4.7).

Mass conservation and s-dynamics. The s-dynamics is no more a pure translation because of the correction term which induces a jump (s stands for the closest site to the moving myosin head), and it is given by the s-marginal $p_t^s := \overline{p}_t^0 + \overline{p}_t^1$. Its evolution can be obtained summing the equations in (4.7):

$$\partial_t p_t^s(s) = -\dot{x}_c(t)\partial_s p_t^s(s) - \dot{x}_c(t)\left[p_0^{\rm th}(d/2|s)\overline{p}_t^0(s) - p_0^{\rm th}(d/2|s+d)\overline{p}_t^0(s+d)\right] \tag{4.10}$$

It isn't a closed equation, and there is no more uniform distribution for s since it now lives in the whole real line $\mathbb{R}$. The mass conservation

$$\int_{\mathbb{R}} \overline{p}_t^0 + \int_{\mathbb{R}} \overline{p}_t^1 = 1$$

can be recovered by integration over s, since

$$\int_{\mathbb{R}} p_0^{\rm th}(d/2|s)\overline{p}_t^0(s)\mathrm{d}s - \int_{\mathbb{R}} p_0^{\rm th}(d/2|s+d)\overline{p}_t^0(s+d)\mathrm{d}s = 0\,, \tag{4.11}$$

using a change of variable.

Detailed balance conditions. The energies driving the dynamics (3.1) were $w_0(x)$ and $w_1(s)$, w_0 being a function of $x = s - h$. To use the s variable as the only parameter for the dynamics, w_0 has to be replaced by a suitable energy functional $\overline{w}_0(s)$. Since h has been thermalized, s is considered as the leading reaction coordinate, and it is natural to consider the related free energy

$$\overline{w}_0(s) := -k_B T \ln Z_0(s)$$

together with the attached-state energy $\overline{w}_1(s) := w_1(s)$. The energy w_0 was involved in the detailed balance condition for jump rates $k_+\left(s-\overline{h},h\right)$ and $k_-^{\rm rev}(s-\overline{h},h)$, together with kernels $\overline{k}_-(s,h)$ and $\overline{k}_+^{\rm rev}(s,h)$, and the compatibility of $\overline{w}_0$ with the new jump rates $\int_{\mathbb{T}_d} k_+(s,h)p_0^{\rm th}(h|s)\mathrm{d}h$, $\int_{\mathbb{T}_d} k_-^{\rm rev}(s,h)p_0^{\rm th}(h|s)\mathrm{d}h$, $\int_{\mathbb{T}_d} \overline{k}_-(s,h)\mathrm{d}h$ and $\int_{\mathbb{T}_d} \overline{k}_+^{\rm rev}(s,h)\mathrm{d}h$ must now be checked. The previous w_0-related detailed balance conditions (3.7) and (3.6) now read

$$\overline{k}_+^{\rm rev}(s,h) = \exp\left[-\frac{w_0\left(s-h\right) - w_1\left(s\right)}{k_B T}\right] k_+(s,h)$$

$$\overline{k}_-(s,h) = \exp\left[-\frac{w_0\left(s-h\right) - w_1\left(s\right) - \mu_T}{k_B T}\right] k_-^{\rm rev}(s,h)$$

To recover the rate (4.6), it is natural to integrate over h. Using the definitions (4.4) and (4.5):

$$\begin{aligned}\int_{\mathbb{T}_d} \overline{k}_+^{\rm rev}(s,h)\mathrm{d}h &= Z_0(s)\exp\left[\frac{w_1\left(s\right)}{k_B T}\right]\int_{\mathbb{T}_d} k_+(s,h)p_0^{\rm th}(h|s)\mathrm{d}h \\ &= \exp\left[-\frac{\overline{w}_0(s) - \overline{w}_1\left(s\right)}{k_B T}\right]\int_{\mathbb{T}_d} k_+(s,h)p_0^{\rm th}(h|s)\mathrm{d}h\end{aligned}$$

and similarly

$$\int_{\mathbb{T}_d} \overline{k}_-(s,h)\mathrm{d}h = \exp\left[-\frac{\overline{w}_0(s) - \overline{w}_1\left(s\right) - \mu_T}{k_B T}\right]\int_{\mathbb{T}_d} k_-^{\rm rev}(s,h)p_0^{\rm th}(h|s)\mathrm{d}h$$

and this gives desired detailed balance conditions with respect to $\overline{w}_0$, which must be satisfied by the components of (4.6).

Energy balance. Let's now compute the time-derivative of the internal energy

$$\mathcal{U}(t) := \int_{\mathbb{R}} \left[\overline{w}_0\left(s\right)\overline{p}_t^0(s) + \overline{w}_1\left(s\right)\overline{p}_t^1(s)\right]\mathrm{d}s$$

to recover the first principle of thermodynamics. The contributions are the same as in section 2.1, except for the contribution due to the correction term, which gives:

$$\begin{aligned}
-\dot{x}_c(t)\int_{\mathbb{R}}\overline{w}_0(s)\left[p_0^{\mathrm{th}}(d/2|s)-p_0^{\mathrm{th}}(d/2|s+d)\right]\overline{p}_t^0(s)\mathrm{d}s&\\
&=-\dot{x}_c(t)\int_{\mathbb{R}}\overline{w}_0(s)\left[p_0^{\mathrm{th}}(d/2|s)-p_0^{\mathrm{th}}(-d/2|s)\right]\overline{p}_t^0(s)\mathrm{d}s\\
&\quad-\dot{x}_c(t)\int_{\mathbb{R}}\overline{w}_0(s)\left[p_0^{\mathrm{th}}(-d/2|s)-p_0^{\mathrm{th}}(d/2|s+d)\right]\overline{p}_t^0(s)\mathrm{d}s\\
&=-\dot{x}_c(t)\int_{\mathbb{R}}-k_BT\ln Z_0(s)\left[-\partial_s\ln Z_0(s)\right]\overline{p}_t^0(s)\mathrm{d}s\\
&\quad-\dot{x}_c(t)\int_{\mathbb{R}}\exp\left[-\frac{w_0(s-d/2)}{k_BT}\right]\left[\frac{\overline{p}_t^0(s)}{Z_0(s)}-\frac{\overline{p}_t^0(s-d)}{Z_0(s-d)}\right]\mathrm{d}s\,,
\end{aligned}$$

using the identity

$$\partial_s Z_0(s)=\int_{-d/2}^{d/2}-\partial_h\exp\left[-\frac{w_0\left(s-h\right)}{k_BT}\right]=-Z_0(s)\left[p_0^{\mathrm{th}}(d/2|s)-p_0^{\mathrm{th}}(-d/2|s)\right]\,.$$

Finally, the first principle reads

$$\begin{aligned}
\frac{\mathrm{d}}{\mathrm{d}t}\mathcal{U}(t)=&\ \dot{x}_c(t)\int_{\mathbb{R}}\partial_s\left[\overline{w}_0(s)-\frac{\overline{w}_0^2(s)}{2k_BT}\right]\overline{p}_t^0(s)\mathrm{d}s\\
&-\dot{x}_c(t)\int_{\mathbb{R}}\exp\left[-\frac{w_0(s-d/2)}{k_BT}\right]\left[\frac{\overline{p}_t^0(s)}{Z_0(s)}-\frac{\overline{p}_t^0(s-d)}{Z_0(s-d)}\right]\mathrm{d}s\\
&+\dot{x}_c(t)\tau_c(t)+\dot{\mathcal{E}}(t)-\int_{\mathbb{R}}\left[\overline{w}_0(s)-\overline{w}_1(s)\right]\left[k_+(s)\overline{p}_t^0(s)-\overline{p}_t^1(s)\int_{\mathbb{T}_d}\overline{k}_+^{\mathrm{rev}}(h',s)\mathrm{d}h\right]\mathrm{d}s\\
&-\int_{\mathbb{R}}\left[\overline{w}_1(s)+\mu_T-\overline{w}_0(s)\right]\left[\overline{p}_t^1\left(s\right)\int_{\mathbb{T}_d}\overline{k}_-(h',s)\mathrm{d}h'-k_-^{\mathrm{rev}}(s)\overline{p}_t^0(s)\right]\mathrm{d}s
\end{aligned}$$

The power of external efforts

$$\dot{\mathcal{W}}(t):=\dot{x}_c(t)\tau_c(t)+\int_{\mathbb{R}}\partial_s\left[\overline{w}_0(s)-\frac{\overline{w}_0^2(s)}{2k_BT}\right]\overline{p}_t^0(s)\mathrm{d}s$$

is the energy required for the displacement of the myosin head in the energy landscape $\overline{w}_1(s)$ and $\overline{w}_0$ (the closest site s to head x now appears, and no more x itself, because s is the only left variable). However, the myosin head x doesn't energetically behave like an actin site because it undergoes a spring-like effort which pulls it back to the origin, and this must be recovered in the dynamics of the closest site s to x. This motivates the quadratic correction to the consumed energy $\overline{w}_0(s)$: less energy is needed since the correction term prevents the head from escaping too far from the origin (this due to the weight $p_0^{\mathrm{th}}(d/2|s)$, see remark 4.4). The second line of the first principle would be zero if the periodicity relation (4.8) were true. However, this not the case, because of the approximation induced by the closure choice (4.4). This energy contribution is thus an artificial extra term due to the approximation error.

Free energy balance. As previously, chemical potentials can be defined by

$$\mu_t^0\left(s\right)=\overline{w}_0(s)+k_BT\ln\overline{p}_t^0(s)\qquad\mu_t^1\left(s\right)=\overline{w}_1\left(s\right)+k_BT\ln\overline{p}_t^1(s)\,,$$

and free energy reads

$$\mathcal{F}(t)=\int_{\mathbb{R}}\mu_t^0(s)\overline{p}_t^0(s)+\mu_t^1(s)\overline{p}_t^1(s)\mathrm{d}s\,.$$

Using mass conservation, its time-derivative is

$$\frac{\mathrm{d}}{\mathrm{d}t}\mathcal{F}(t)=\int_{\mathbb{R}}\mu_t^0\left(s\right)\partial_t\overline{p}_t^0(s)+\mu_t^1\left(s\right)\partial_t\overline{p}_t^1(s)\mathrm{d}s\,.$$

All the computations for the Huxley system have been done previously in section 2.1, and the only difference when using (4.7) comes from the correction term which adds the contribution

$$-\dot{x}_c(t)\int_{\mathbb{R}}\mu_t^0(s)\left[p_0^{\text{th}}(d/2|s)-p_0^{\text{th}}(d/2|s)\right]\overline{p}_t^0(s+d)\mathrm{d}s$$

Since $\overline{w}_0(s)=-k_BT\ln Z_0(s)$, one gets $\mu_t^0(s)=k_BT\ln\left[Z_0^{-1}(s)\overline{p}_t^0(s)\right]$ and the above term reads

$$-\dot{x}_c(t)k_BT\int_{\mathbb{R}}\exp\left[-\frac{w_0(s-d/2)}{k_BT}\right]\ln\left[\frac{\overline{p}_t^0(s)}{Z_0(s)}\left(\frac{\overline{p}_t^0(s-d)}{Z_0(s-d)}\right)^{-1}\right]\mathrm{d}s\,.$$

At this point, we see the effect of the approximation which has been made to obtain the closed system (4.7). If the periodicity relation (4.8) were true, this writing shows that the above contribution would vanish (as expected from this mass re-equilibrium term which is a writing artifact and doesn't correspond to any physical jump). However, this relation isn't true because of the closure choice (4.4) which only leads to an approximation of (4.2). This approximation introduces an additional entropy contribution, which would be zero in the exact setting (maybe cleverer closure choices allow to keep this features, but then the authors didn't manage to find them). Moreover, the sign of this contribution depends on the one $\dot{x}_c(t)$, and this doesn't permit a systematical accordance with the Second Law.

Remark 4.7 (Towards a correction of the free energy balance). Although it seems difficult to remove the term in this balance due to the approximation error, it would be satisfying to make its sign respect the second Law. To do so, one could think about adding a reverse jump to the dynamics, which would compensate its effect. Such a possible correction is to consider

$$\begin{array}{rl}\partial_t\overline{p}_t^0(s)= & -\dot{x}_c(t)\left[p_0^{\text{th}}(d/2|s)\overline{p}_t^0(s)-p_0^{\text{th}}(d/2|s+d)\overline{p}_t^0(s+d)\right]\\ & -\dot{x}_c(t)\left[p_0^{\text{th}}(-d/2|s)\overline{p}_t^0(s)-p_0^{\text{th}}(-d/2|s-d)\overline{p}_t^0(s-d)\right]\\ & -\dot{x}_c(t)\partial_s\overline{p}_t^0(s)-f(s)\overline{p}_t^0(s)+g(s)\overline{p}_t^1(s)\end{array},$$

which leads to the entropy contribution in the free energy

$$\int_{\mathbb{R}}\left[\mu_t^0(s-d)-\mu^0(s)\right]\left[p_0^{\text{th}}(d/2|s)\overline{p}_t^0(s)-p_0^{\text{th}}(-d/2|s-d)\overline{p}_t^0(s-d)\right]\leq 0\,.$$

Provided $\dot{x}_c(t)\leq 0$, this is indeed non-positive because of the detailed balance condition:

$$\frac{\overline{p}_t^0(s)}{\overline{p}_t^0(s-d)}=\frac{Z_0(s-d)}{Z_0(s)}=\exp\left[-\frac{\overline{w}_0(s-d)-\overline{w}_0(s)}{k_BT}\right].$$

However, the physical relevance of this ratio remains unclear, because privileging either the jump $s\to s-d$ or $s\to s+d$ to re-equilibrate mass seems quite arbitrary.

5. **Numerical illustrations**

We now present a calibration of our newly introduced hierarchy of models and show its capability to reproduce key indicators of the cardiac muscle contraction physiology. Our target for the calibration is two categories of fundamental physiological modes of contraction: the isometric contraction – contraction mode in which the relative sliding of the actin and myosin filament is prevented in the experimental setup – and the steady-state contraction at constant shortening velocity. More precisely, we target the ratio of attached myosin heads and the force per attached myosin head during isometric contraction and the force-velocity curve in steady-state conditions (where the macroscopic force T is normalized that the isometric macroscopic force T_0, see Figure 4). These two modes of contraction have historically been used to characterize the behavior of muscles [21] and are key features of the physiology at the heart level in the isovolumetric contraction phase and ejection phase, respectively.

5.1. **Model calibration**

To calibrate the models, one needs to provide the actin inter-site distance d, the attached and detached state energy potential $w_1(x)$ and $w_0(x)$ and the attachment rates $k_+(x,h)$ and $k_-^{rev}(x,h)$.

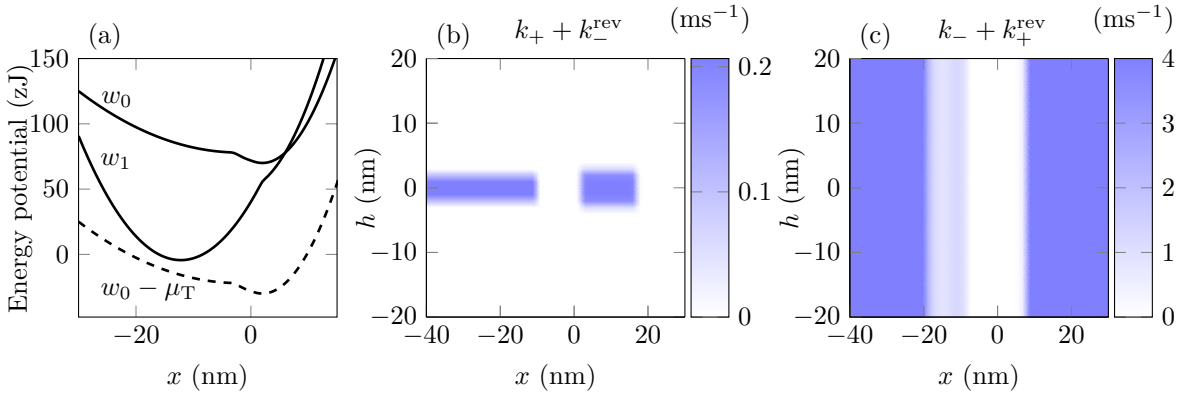

FIGURE 4. h-model parameter functions. (a) Attached energy potential w_1 and detached energy potential w_0. (b) Attachment rate. (c) Detachment rate. Expressions and parameters values can be found in Table. 2.

Note that the detachment rates $k_+(x,h)$ and $k_-^{rev}(x,h)$ result from the attachment rates and energy potentials through the detailed balance equations (3.6) and (3.7).

We describe here the main principles that have guided the calibration process. A detailed presentation of the chosen model elements expressions and the model parameters values is given in Table 2 and illustrated in Figure 4 for the h-model and in Figure 6 for the h-reduced model.

The actin filament is made of a double helix of actin monomers that is covered by tropomyosin proteins whose length corresponds to the helix periodicity and which drive the muscle activation by uncovering the actin sites [34]. This gives rise to two paradigms that are both used in the literature for the choice of the inter-site distance: the actin filament helix periodicity ($\sim$40 nm) [15, 52, 54, 38, 8, 31] – this paradigm is selected in this paper – or the size of the actin monomer ($\sim$5.5 nm) [47, 3].

The chosen isometric indicators – the ratio of attached heads $\check{n}_a$ and the force per attached head $\check{\tau}_c$ – bring constraints on the transitions rates and the attached energy potential. These indicators for the h-model are given by

$$\check{n}_a = \int_{\mathbb{R}} p_\infty(x,1)\mathrm{d}x, \qquad \text{and} \qquad \check{\tau}_c = \frac{1}{\check{n}_a}\int_{\mathbb{R}} \partial_x w_1(x) p_\infty(x,1)\mathrm{d}x,$$

where $p_\infty(x,1) = \lim_{t\to\infty} p_t(x,1)$ in isometric conditions ($\dot{x}_c = 0$). On the one hand, the ratio of attached heads is driven by the attachment-detachment process and thus the associated rates. On the other hand, as with the Huxley–Hill model family, the model produces a positive active force τ_c by having myosin heads attached in a stretched configuration. The force per attached head thus constraints the choice of the myosin heads attached stiffness and the attachment rate so that attachment is favored in regions where positive force is generated.

The reduction of macroscopic force with the sliding velocity in a steady-state contraction, which is summarized by the classical force-velocity curve, results from the competition between force reduction due to variations of the attached myosins extension and the cycling process. Indeed, the filament sliding moves the attached myosin heads towards a compression range where they potentially contribute negatively to the macroscopic force ($\tau_c < 0$). The detachment process allows these counter-productive myosin heads to detach and to re-attach in a position where they now contribute positively to the macroscopic force ($\tau_c > 0$).

The attachment rate is thus set so that myosin heads can attach when x lies in an interval of positive values and when they are close to their nearest actin site, i.e. when h belongs to a limited interval in absolute value, see Figure 4 (b). Following recent works [8, 31, 45], we choose a regularized double well potential for the attached potential w_1, see Figure 4 (a). Few experimental data are available to guide the calibration of the detached potential w_0. We thus choose the same form as the attached potential and set the energy wells such that the detached myosin heads are attracted towards the region where they can attach.

TABLE 1. Isometric physiological indicators: ratio of attached heads and force per attached head. The experimental values are obtained from rat cardiac isometric experiments. The ratio of attached head is taken from [4]. The force per attached head is derived from the data given in [49] considering that the average macroscopic force scale linearly with the ratio of attached heads.

Isometric indicators	Experiments	h-model	h-reduced model
Ratio of attached heads	0.15	0.150	0.276
Force per attached head	6.14 pN	6.28 pN	5.73 pN

Given the constraints brought by the isometric indicators, the force-velocity curve will mainly add constraints on the detachment rates imposing that the myosins detach when they operate in compression. Given the detailed balance relation (3.7), this translates into the definition of k_-^{rev} as a non-zero function when h belongs to a limited interval in absolute value and the myosin head is in compression, see Figure 4(c).

5.2. h-model

We first present the results obtained with the h-model. Equations (3.1) are simulated with a standard Euler-Maruyama method for the transport, drift and diffusion terms [10] and the scheme presented in Appendix A for the jump terms. The isometric indicators (obtained with $\dot{x}_c = 0$) are summarized in Table 1. The force-velocity curve is presented in Figure 5.

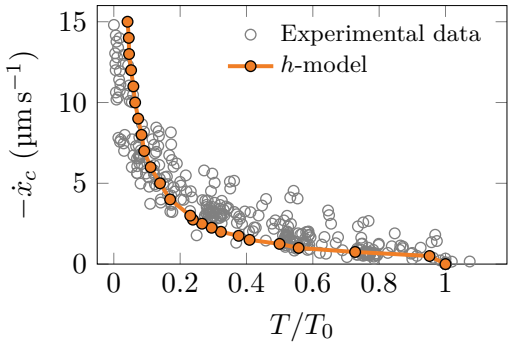

FIGURE 5. Evaluation of the calibrated h-model prediction against experimental data. Experimental data are obtained with rat cardiac intact muscles cells around 25 °C, see [33] Figure 4(a) for more details. Note that for low shortening velocities ($\dot{x}_c < 0.5\,\mu\text{m}\,\text{s}^{-1}$), experimental data display instabilities [12, 13, 56, 19], which are classically the subject of dedicated experimental investigations. Reproducing this behavior is out of the scope of this paper. Model predictions is this regime are thus not considered.

The physiological indicators simulated with the h-model show a good agreement with the experiment data.

5.3. h-reduced model

To assess the impact of the modeling assumptions used to derive the h-reduced model (see Section 4.2), we compare the model predictions against that of the h-model. The h-reduced model parameters functions and parameters – energy potentials, transition rates, ... – are straightforwardly determined through the model reduction process, see Section 4.2. To assess the impact of the modeling assumptions used to derive the h-reduced model (see Section 4.2), we compare the model predictions against that of the h-model. The h-reduced model parameters functions and parameters – energy potentials, transition rates, ... – are straightforwardly determined through the model reduction process, see Section 4.2. They are presented in Figure 6. One can note that

the detached energy potential appears naturally in the model reduction process as a flat function in the range of "moderate" values of the variable s. This can be related to the Huxley–Hill models, in which the detached potentials are constants.

The physiological indicators of the h-reduced model are given by

$$\check{n}_a = \int_{\mathbb{R}} \overline{p}_\infty(s,1)\mathrm{d}s, \qquad \text{and} \qquad \check{\tau}_c = \frac{1}{\check{n}_a}\int_{\mathbb{R}} \partial_s \overline{w}_1(s)\overline{p}^1_\infty(s)\mathrm{d}s,$$

where $\overline{p}^1_\infty(s) = \lim_{t\to\infty} \overline{p}^1_t(s)$ in isometric conditions ($\dot{x}_c = 0$). Table 1 presents a comparison of the physiological indicators and Figure 7 of the force-velocity relation.

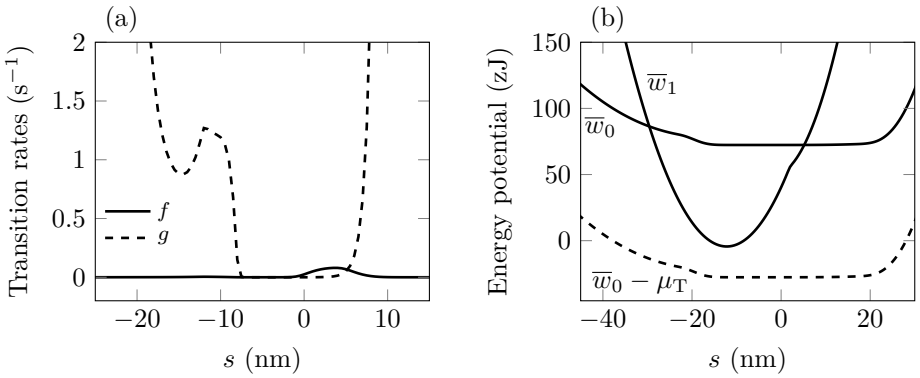

Figure 6. h-reduced model parameter functions. (a) Attached energy potential $\bar{w}_1$ and detached energy potential $\bar{w}_0$. (b) Transitions rates.

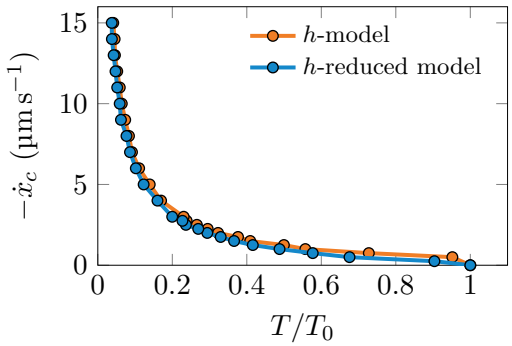

Figure 7. Comparison of the force-velocity for the relative coordinate model and the Huxley generalized reduced model.

The ratio of attached heads of the h-reduced model displays a 84 % increase in comparison with the h-model while the forces per attached heads remain close to each other and the normalized force-velocity curves of the two models also show a good agreement. This means that the reduced model favors more the attachment of myosin heads but that the behavior of attached heads is relatively unaffected by the model reduction process. This can be explained by the fact that the thermalization procedure used to obtain the attachment rate f is a convolution operator that spreads the support of the function f compared to that of k_+ allowing attachment in a region where the detachment rate g is very low thus favoring the attached configuration compared to the h-model. The calibration should be fine-tuned so that the detachment rate baseline is higher in this region.

6. Conclusion

In this work, we introduced a novel modeling framework of the acto-myosin interaction, which represents an alternative to the seminal Huxley–Hill framework. A jump-diffusion stochastic

model is proposed. It describes the myosin state by its attachment state, the extension of the myosin neck and the distance to the nearest actin site relatively to the current myosin tip position. Unlike Huxley–Hill formulations, which describe the actin site from the anchor position, no restriction of the myosin extension in the detached state must be imposed. The new framework thus accounts for a wider class of physiological configurations without resorting to a more complex multi-site framework. A reduced version is derived from an adiabatic elimination of fast variables. This reduced model can be seen as an extension of the Huxley–Hill framework to the full real line, independently of the inter-site distance. The compatibility of both newly introduced models with the thermodynamics principles is established at each step of the models' derivation.

With its eulerian parametrization being closer to the actual molecular configuration, our novel framework paves the way to the introduction of modeling bricks that capture refined molecular features of the actin-myosin interaction.

Appendix A. About jump processes and Poisson random measures

This section provides some (non-rigorous) mathematical reminders: it briefly explains to a reader, maybe not familiar with these mathematical notions, how to model jump processes using Poisson random measures, and how their generator can be recovered from them.

A.1. Pure jump process and their numerics

Given a measured (state) space E, a pure Markov, càdlàg (i.e. right-continuous with left-limits), pure jump process $(\alpha_t)_{t\geq 0}$ can be built from the specification of:

- A rate function k, which dictates the frequency of jumps.
- A jump probability measure $K\left(x, \mathrm{d}x'\right)$ which dictates, at a jumps time t, the law of the (random) choice of the value $\alpha_t = x'$, starting from $\alpha_{t^-} = x$ just before the jump.

The convention is adopted here to tag the arrival variables with a prime. Let p_t be the law of α_t at time t, i.e. the probability measure on E which quantifies the likelihood of values taken by α_t. For regular test functions φ (see e.g. [35] for rigorous definitions and justifications), one then has

$$\frac{\mathrm{d}}{\mathrm{d}t}\mathbb{E}\left[\varphi\left(\alpha_t\right)\right] = \frac{\mathrm{d}}{\mathrm{d}t}\int_E \varphi \,\mathrm{d}p_t = \int_E L\varphi \,\mathrm{d}p_t = \mathbb{E}\left[L\varphi\left(X_t\right)\right] , \tag{A.1}$$

the operator L being the *infinitesimal generator* of the Markov process $(\alpha_t)_{t\geq 0}$. It is defined by

$$L\varphi(x) = k(x)\int \left[\varphi(x') - \varphi(x)\right] K(x, \mathrm{d}x')$$

Using the duality measure-function, one can define a dual operator $L^\star$ on measures by

$$\int_E \varphi \mathrm{d}\left(L^\star p_t\right) := \int_E L\varphi \mathrm{d}p_t$$

Since

$$\begin{aligned}\mathbb{E}\left[L\varphi\left(\alpha_t\right)\right] &= \int_E k(x)\int_E \left[\varphi\left(x'\right) - \varphi\left(x\right)\right] K\left(x, \mathrm{d}x'\right) p_t\left(\mathrm{d}x, \mathrm{d}\alpha\right) \\ &= -\int_E \varphi\left(x\right) k\left(x\right) p_t\left(\mathrm{d}x\right) + \int_E \varphi\left(x'\right)\left(\int_E k(x) K\left(x, \mathrm{d}x'\right) p_t\left(\mathrm{d}x\right)\right)\end{aligned}$$

one gets

$$L^\star p_t\left(\mathrm{d}x\right) = -k\left(x\right) p_t\left(\mathrm{d}x\right) + \int_E k(x') K\left(x', \mathrm{d}x\right) p_t\left(\mathrm{d}x'\right)$$

Equations (A.1) gives the dual master equation

$$\frac{\mathrm{d}}{\mathrm{d}t}p_t = L^\star p_t$$

In case $E = \mathbb{R}$, when both $p_t(\mathrm{d}x) = p_t(x)\mathrm{d}x$ and $K(x, \mathrm{d}x') = K(x, x')\mathrm{d}x'$ admit a density with respect to the Lebesgue measure, this is the integral equation governing the evolution of p_t:

$$\partial_t p_t(x) = -k(x)p_t(x) + \int_E k(y)K(x', x)p_t(x')\mathrm{d}x'$$

Seeing $p_t(x)\mathrm{d}x$ as the number of individual agents in the state x, this means that during a time interval $\mathrm{d}t$:

- A fraction $k(x)\mathrm{d}t$ of these agents jump to another state.
- For each x', a fraction $k(x')K(x', x)$ of the agents in state x' jump to the state x.

These behaviours correspond to each term of the evolution equation.

To perform some Monte-Carlo simulation of the density p_t, one needs to simulate N independent realizations $\alpha_t^1, \dots, \alpha_t^N$ of the process α_t, to then write

$$\mathbb{E}\left[\varphi\left(\alpha_t\right)\right] \simeq \frac{1}{N}\sum_{i=1}^{N} \varphi\left(\alpha_t^i\right)$$

following the law of large numbers. To build such a realization α_t^i, it is possible to use a *Poisson clock*, which counts the number of occurrences of independent events with exponentially distributed waiting time (see [10]). Consider indeed a sequence $(e_n)_{n\in\mathbb{N}}$ of independent unit exponential random variables. The sequence $(T_n)_{n\in\mathbb{N}}$ of jump times for the process $(X_t)_{t\geq 0}$ is then defined by induction from this jump clock: initializing at $T_0 = 0$, the $(n+1)$-th jump time knowing the n-th is given by

$$T_{n+1} = \inf\left\{t > T_n\,,\, k\left(\alpha_{T_n}\right)(t - T_n) \geq e_n\right\} \tag{A.2}$$

At the jump time T_{n+1}, the value of $\alpha_{T_{n+1}}$ is then chosen according to the jump measure $K\left(\alpha_{T_n}, \mathrm{d}x\right)$. This algorithm provides numerical simulations for α_t, but it doesn't give a compact representation of the process by an equation. More precisely, one would like a continuous object which describes the increment $\mathrm{d}\alpha_t$ of α_t at time t, using its most recent past value α_{t^-}. The adequate tool is the quite theoretical notion of Poisson random measure, whose formal definition is sketched in next subsection.

A.2. **Poisson random measures**

Detailed mathematical references for the content of this section can be found in e.g. [29],[**?**] or [1]. Let us fix a filtered probability space $(\Omega, \mathcal{F}, (\mathcal{F}_t)_t, \mathbb{P})$.

Definition A.1 (Poisson random measure)**.** Let (E, μ) be a measurable Polish with a σ-finite measure μ on the borelian σ-algebra. A Poisson random measure with intensity μ is a random variable N on Ω with values in the set of probability measures on E such that:

(1) For each $\omega \in \Omega$, $N(\omega, \cdot)$ is a finite measure which can be expressed as a countable sum of Dirac measures.

(2) The mapping $\omega \in \Omega \mapsto N(\omega, A)$ is measurable for any measurable set A which is μ-finite.

(3) For disjoints measurable and μ-finite sets $A_1, \dots, A_k$, the random variables $N(A_j)$, for $1 \leq j \leq k$ are independent, and $N(A_j)$ obeys a Poisson law on $\mathbb{N}$ with parameter $\mu(A_j)$.

Let's only consider the case $E = \mathbb{R}_+ \times \mathcal{U}$ and $\mu(\mathrm{d}t, \mathrm{d}u) = \mathrm{d}t \otimes \nu(\mathrm{d}u)$, for some parameter space $\mathcal{U}$. To write stochastic differential equations, the Poisson random measure N is assumed to be *adapted*, i.e:

(1) $N(A)$ is $\mathcal{F}_t$-measurable for each measurable set $A \subset [0, t] \times \mathcal{U}$, for $t > 0$

(2) The σ-field generated by $\{N(A),\ A \subset [0, t] \times \mathcal{U}$ measurable $\}$ is independent of $\mathcal{F}_t$.

When $\nu(\mathcal{U}) < +\infty$, $(N((0,t]\times\mathcal{U}))_{t\geq 0}$ is a classical Poisson process with parameter $\nu(\mathcal{U})$, and N can be shown to admit the representation:

$$N(\mathrm{d}t, \mathrm{d}u) = \sum_{n=1}^{M} \delta_{(T_n,u_n)}(\mathrm{d}t, \mathrm{d}u),$$

where M is the (random) number of jumps in the interval $(0,t]$, and $T_1,\dots,T_M$ are the jump times of $N_t(\mathcal{U})$; the u_i are moreover i.i.d. variables with common law $\nu(\mathrm{d}u)/\nu(\mathcal{U})$. For a measurable function $\varphi : \mathbb{R}_+ \times \mathcal{U} \to \mathbb{R}$, the integral of φ against N is then defined as

$$\int_0^T \int_{\mathcal{U}} \varphi(s,u) N(\mathrm{d}s, \mathrm{d}u) := \sum_{n=1}^{M} \varphi(T_n, u_n).$$

This integral is thus the sum of the random amplitudes $\varphi(T_n,u_n)$ at each jumping time T_n, and this still holds when φ is a random function (i.e. φ additionally depends on ω). This construction can be extended to parameter sets $\mathcal{U}$ with σ-finite ν-measure, provided some L^1 bound assumption:

$$\mathbb{E}\left[\int_0^t \int_{\mathcal{U}} |\varphi(s,u)| \nu(\mathrm{d}u)\mathrm{d}s\right] < +\infty$$

The natural framework for these measures (and more generally stochastic integration) is a L^2 bound assumption, but this goes beyond the scope of what is needed here (see the aforementioned references for rigorous constructions). A property inherited from the construction is the fact that

$$\int_0^t \int_{\mathcal{U}} \varphi(s,u) N(\mathrm{d}s, \mathrm{d}u) - \int_0^t \int_{\mathcal{U}} \varphi(s,u)\nu(\mathrm{d}u)\mathrm{d}s,$$

is a $\mathcal{F}_t$-martingale (in fact, it characterizes N). As a consequence, a process $(\alpha_t)_{t\geq 0}$ defined by the stochastic equation

$$\alpha_t = \int_0^t \int_{\mathcal{U}} c(\alpha_{s^-}, u) N(\mathrm{d}s, \mathrm{d}u)$$

is a Markov process with generator

$$L\varphi(x) = \int_{\mathcal{U}} \left[\varphi(x + c(x,u)) - \varphi(x)\right] \nu(\mathrm{d}u)$$

and the definition of α_t can be re-written as

$$\mathrm{d}\alpha_t = \int_{\mathcal{U}} c(\alpha_{t^-}, u) N(\mathrm{d}t, \mathrm{d}u) \tag{A.3}$$

which is a stochastic differential equation(SDE).

Remark A.2 (Case of absolutely continuous jump measures). If instead one wants to build a Markov process whose generator is given by a kernel $(x,y) \mapsto \overline{k}(x,y)$ such that

$$L\varphi(x) = \int_{\mathbb{R}} \left[\varphi(x + c(x,x')) - \varphi(x)\right] \overline{k}(x,x')\mathrm{d}x'$$

it is sufficient to consider a Poisson random measure on $\mathbb{R}_+ \times \mathbb{R}_+ \times \mathbb{R}$ with intensity measure $\mathrm{d}t \otimes \mathrm{d}u \otimes \mathrm{d}x'$. The jump term to consider in the right-hand side of the SDE is then (A.3)

$$\int_{\mathbb{R}_+\times\mathbb{R}} c(\alpha_{t^-}, x') \mathbb{1}_{u \leq \overline{k}(X_{t^-}, x')} N(\mathrm{d}t, \mathrm{d}u, \mathrm{d}x')$$

This is used in all the document, and the related instantaneous jump rate is then the normalization constant

$$k(x) = \int_{\mathbb{R}} \overline{k}(x,x')\mathrm{d}x'$$

so that in the formalism of the previous subsection, the jump measure is $K(x,\mathrm{d}x') = \frac{\overline{k}(x,x')\mathrm{d}x'}{k(x)}$: the bar notation refers to the fact the kernel $\overline{k}$ is non-normalized. For numerical purposes, the adequate description (A.2) of jump times now reads [10]

$$T_{n+1} = \inf\left\{t > T_n\,,\ \int_{T_n}^t \int_{\mathbb{R}} c(\alpha_{s^-}, x)\mathrm{d}x'\mathrm{d}s \geq e_n\right\}$$

This method will also work for simulating jump-diffusion processes (see next subsection).

A.3. **Jump-diffusion processes**

Adding the previous jump mechanism on a usual (overdamped Langevin) diffusion leads to SDEs in $\mathbb{R}^d$ of the kind:

$$X_t = X_0 + \int_0^t b(X_s)\mathrm{d}s + \int_0^t \sigma(X_s)\mathrm{d}B_s + \int_0^t \int_{\mathcal{U}} c(X_{s^-}, u)N(\mathrm{d}s, \mathrm{d}u) \tag{A.4}$$

with $c : \mathbb{R}^d \times \mathcal{U} \to \mathbb{R}^d$. Assume the following Lipschitz integrability conditions:

(1) For all $x \in \mathbb{R}^d$ and $T > 0$, $\int_0^T \int_{\mathcal{U}} |\alpha(x,u)|\nu(\mathrm{d}u) < +\infty$.

(2) There exists $C > 0$ such that for any $x, y \in E$,
$$|\sigma(x) - \sigma(y)|^2 + |b(x) - b(y)|^2 \leq C|x-y|^2.$$

(3) The L^1 bound holds
$$\int_{\mathcal{U}} |\alpha(x,u) - \alpha(y,u)|\nu(\mathrm{d}u) \leq C|x-y|$$

In this L^1 setting, strong existence and uniqueness for the SDE (A.4) are proven in [18, Theorem 1.2]. Moreover, the generator of the process is the sum of the two generators

$$L_{\text{diffusion}}\varphi(x) = \sum_{i=1}^d b(x)\cdot\nabla\varphi(x) + \frac{1}{2}\sum_{i,j=1}^d (\sigma\sigma^{\mathrm{T}})_{ij}(x)\partial_{x_i}\partial_{x_j}\varphi(x),$$
$$L_{\text{jumps}}\varphi(x) = \int_{\mathcal{U}} \big\{\varphi\big(x + c(x,u)\big) - \varphi(x)\big\}\nu(\mathrm{d}u)$$

This well-posedness result is used in Section 3.1 to build the relative coordinate model.

Appendix B. **Free energy balance and detailed balance**

This section summarizes the general computations which show how detailed balance conditions guaranty the non-negativity of produced entropy. Assume $((\alpha_t, X_t))_{t\geq 0}$ to be a general $\{0,1\}\times E$-valued pure jump process whose marginal law a time t reads

$$\left[\mathbb{1}_{\alpha=0}p_t(x,0) + \mathbb{1}_{\alpha=1}p_t(x,0)\right]\mathrm{d}\alpha\mathrm{d}x \in \mathcal{P}\left(\{0,1\}\times E\right)$$

admits a density with respect to $\mathrm{d}\alpha\mathrm{d}x$ for a given measure $\mathrm{d}x$ on E. This process is assumed to obey two possible jumps:

- A jump $0 \to 1$ for α which occurs at rate $k(x)$, and causes a jump for x with jump law $K(x, \mathrm{d}x')$.
- A reverse $1 \to 0$ for α which occurs at rate $k^{\text{rev}}(x)$, and causes a jump for x with jump law $K^{\text{rev}}(x, \mathrm{d}x')$.

As in section 2.1, assume an energy function $w(\alpha, x) = \mathbb{1}_{\alpha=0}w_0(x) + \mathbb{1}_{\alpha=1}w_1(x)$ is associated to the system (w_α is the energy related to the state α). The chemical potentials at time t are then defined as

$$\mu_t(\alpha, x) := w(\alpha, x) + k_B T \ln p_t(x,\alpha)\,(x,t) = \mathbb{1}_{\alpha=0}\mu_t^0(x) + \mathbb{1}_{\alpha=1}\mu_t^1(x)$$

where the state chemical potentials at time t are

$$\mu_t^0(x) = w_0(x) + k_B T \ln p_t(x,0)\,(x,t) \qquad \mu_t^1(x) = w_1(x) + k_B T \ln p_t(x,1)\,(x,t)$$

Free energy is then defined as

$$\mathcal{F}(t) := \int_E \left[\mu_t^0(x)p_t(x,0) + \mu_t^1(x)P_t(x,1)\right]\mathrm{d}x$$

Using the formalism of appendix A.1 for pure jump processes, the time-derivative of $\mathcal{F}(t)$ reads

$$\begin{aligned}\frac{\mathrm{d}}{\mathrm{d}t}\mathcal{F}(t) = &\int_E -\mu_t^0(x)\,k(x)\,p_t(x,0)\,\mathrm{d}x + \int_E \mu_t^0(x)\int_E k^{\mathrm{rev}}(x')K^{\mathrm{rev}}\left(x',\mathrm{d}x\right)p_t\left(x',1\right)\mathrm{d}x'\\ &+\int_E -\mu_t^1(x)\,k^{\mathrm{rev}}(x)\,p_t(x,1)\,\mathrm{d}x + \int_E \mu_t^1(x)\int_E k(x')K\left(x',\mathrm{d}x\right)p_t\left(x',0\right)\mathrm{d}x'\end{aligned}$$

Since jump measures are probability measures, the following normalization conditions hold

$$\int_E K\left(x,\mathrm{d}x'\right)=1 \qquad \int_E K^{\mathrm{rev}}\left(x',\mathrm{d}x\right)=1$$

Switching names of dumb variables, this leads to

$$\begin{aligned}\frac{\mathrm{d}}{\mathrm{d}t}\mathcal{F}(t) =& \int_E -\mu_t^0(x)\,k(x)\int_E K\left(x,\mathrm{d}x'\right)p_t(x,0)\,\mathrm{d}x + \int_E \mu_t^1\left(x'\right)\int_E k(x)K\left(x,\mathrm{d}x'\right)p_t(x,0)\,\mathrm{d}x\\ &+\int_E -\mu_t^1\left(x'\right)k^{\mathrm{rev}}\left(x'\right)\int_E K^{\mathrm{rev}}\left(x',\mathrm{d}x\right)p_t\left(x',1\right)\mathrm{d}x'\\ &+\int_E \mu_t^0(x)\int_E k^{\mathrm{rev}}(x')K^{\mathrm{rev}}\left(x',\mathrm{d}x\right)p_t\left(x',1\right)\mathrm{d}x'\\ =&\int_E\int_E\left[\mu_t^1\left(x'\right)-\mu_t^0(x)\right]k(x)\,K\left(x,\mathrm{d}x'\right)p_t(x,0)\,\mathrm{d}x\\ &+\quad\int_E\int_E\left[\mu_t^0(x)-\mu_t^1\left(x'\right)\right]k^{\mathrm{rev}}(x')K^{\mathrm{rev}}\left(x',\mathrm{d}x\right)p_t\left(x',1\right)\mathrm{d}x'\\ =&\int_E\int_E\left[\mu_t^1\left(x'\right)-\mu_t^0(x)\right]\\ &\qquad\cdot\left[k(x)\,K\left(x,\mathrm{d}x'\right)p_t(x,0)\,\mathrm{d}x - k^{\mathrm{rev}}(x')K^{\mathrm{rev}}\left(x',\mathrm{d}x\right)p_t\left(x',1\right)\mathrm{d}x'\right]\end{aligned}$$

The produced entropy $\dot{S}_{\mathrm{prod}}(t)$ must equal here $-\frac{1}{T}\frac{\mathrm{d}}{\mathrm{d}t}\mathcal{F}(t)$. To satisfy the second law of thermodynamics, the following quantity has to be non-negative

$$\begin{aligned}T\dot{S}_{\mathrm{prod}}(t) = &\int_E\int_E\left[\mu_t^0(x)-\mu_t^1\left(x'\right)\right]\\ &\qquad\cdot\left[k(x)\,K\left(x,\mathrm{d}x'\right)p_t(x,0)\,\mathrm{d}x - k^{\mathrm{rev}}(x')K^{\mathrm{rev}}\left(x',\mathrm{d}x\right)p_t\left(x',1\right)\mathrm{d}x'\right]\end{aligned}$$

If Arrhenius's law is respected, the detailed balance condition holds (in the weak sense of measures)

$$k(x)\,K\left(x,\mathrm{d}x'\right)\mathrm{d}x = \exp\left[-\frac{w_1(x')-w_0(x)}{k_BT}\right]k^{\mathrm{rev}}(x')K^{\mathrm{rev}}\left(x',\mathrm{d}x\right)\mathrm{d}x' \tag{B.1}$$

for the reaction $x\to x'$. Indeed, the measure $k(x)\,K(x,\mathrm{d}x')\,\mathrm{d}x$ is exactly the chemical rate related to the direct sense reaction. At that condition

$$\begin{aligned}T\dot{S}_{\mathrm{prod}}(t) = \int_E\int_E\left[\mu_t^0(x)-\mu_t^1\left(x'\right)\right]&\left[\exp\left(-\frac{w_1(x')-w_0(x)}{k_BT}\right)-\frac{p_t\left(x',1\right)}{p_t(x,0)}\right]\\ &\cdot k^{\mathrm{rev}}(x')K^{\mathrm{rev}}\left(x',\mathrm{d}x\right)p_t(x,0)\,\mathrm{d}x'.\end{aligned}$$

Note now that

$$\begin{aligned}\mu_t^0(x)-\mu_t^1\left(x'\right) &= w_0(x)-w_1(x')+k_BT\ln\left(\frac{p_t(x,0)}{p_t\left(x',1\right)}\right)\\ &= k_BT\ln\left[\exp\left(-\frac{w_1(x')-w_0(x)}{k_BT}\right)\frac{p_t(x,0)}{p_t\left(x',1\right)}\right]\end{aligned}$$

so that $T\dot{S}_{\mathrm{prod}}(t)$ has the sign of the product $\ln(xy)\left[x-\frac{1}{y}\right]$ for positive real numbers x and y. If $x\geq\frac{1}{y}$ then both terms are non-negative since $xy\geq 1$. In the same vein, both terms are negative if $x<\frac{1}{y}$. *Finally, $\dot{S}_{prod}(t)$ is always non-negative, and the entropy balance is respected provided the detailed balance condition* (B.1) *holds.*

Appendix C. Calibration parameters

Table 2. Calibrated model parameters

Parameter	Symbol	Value
Energy potentials (see Figure 4(a))		
Definition of the potential $w_\alpha(x) = \hat{w}_\alpha(x) + E_\alpha$		
$\hat{w}_\alpha(x) = \begin{cases} \kappa_{\alpha,\ell}/2\,(x-\tilde{x}_\alpha,\ell)^2 + \tilde{w}_\alpha & \text{if } x < x_{\alpha,\ell}, \\ \kappa_{\alpha,r}/2\,(x-\tilde{x}_{\alpha,r})^2 & \text{if } x > x_{\alpha,r}, \\ \big[\kappa_{\alpha,\ell}/2\,(x_{\alpha,\ell}-\tilde{x}_{\alpha,\ell})^2 + \tilde{w}_\alpha\big]\phi_1(x) & \\ + \quad \kappa_{\alpha,\ell}\,(x_{\alpha,\ell}-\tilde{x}_{\alpha,\ell})\phi_2(x) & \\ + \quad \big(\kappa_{\alpha,r}/2\,(x_{\alpha,r}-\tilde{x}_{\alpha,r})^2\big)\phi_3(x) & \\ + \quad \kappa_{\alpha,r}\,(x_{\alpha,r}-\tilde{x}_{\alpha,r})\phi_4(x) & \\ + \quad \check{w}_\alpha\phi_5(x) & \text{if } x \in [x_{\alpha,\ell}, x_{\alpha,r}] \end{cases}$	$\kappa_{1,\ell}$ $\kappa_{1,r}$ $\tilde{x}_{1,\ell}$ $\tilde{x}_{1,r}$ x_1 $x_{1,\ell}$ $x_{1,r}$ $\check{w}_1$ E_1	$0.60\,\mathrm{pN\,nm^{-1}}$ $1\,\mathrm{pN\,nm^{-1}}$ $-12.5\,\mathrm{nm}$ $-1.5\,\mathrm{nm}$ $2\,\mathrm{nm}$ $2.5\,\mathrm{nm}$ $1.3\,\mathrm{nm}$ $5.7\,\mathrm{zJ}$ $50\,\mathrm{zJ}$
$\tilde{w}_\alpha = -\kappa_{\alpha,\ell}/2\,(x_\alpha - \tilde{x}_{\alpha,\ell})^2 + \kappa_{\alpha,r}/2\,(x_\alpha - \tilde{x}_{\alpha,r})^2$	$x_{\alpha,r}$	$2\,\mathrm{nm}$
Interpolation functions		
$\begin{cases} \phi_1(x) = (x-x_{\alpha,r})^2/(x_{\alpha,r}-x_{\alpha,\ell})^2 \cdot\Big(2(x-x_{\alpha,\ell})/(x_{\alpha,r}-x_{\alpha,\ell})+1\Big) \\ \phi_2(x) = (x-x_{\alpha,r})^2/(x_{\alpha,r}-x_{\alpha,\ell})^2 \cdot (x-x_{\alpha,\ell}) \\ \phi_3(x) = (x-x_{\alpha,\ell})^2/(x_{\alpha,r}-x_{\alpha,\ell})^2 \cdot\Big(3-2(x-x_{\alpha,\ell})/(x_{\alpha,r}-x_{\alpha,\ell})\Big) \\ \phi_4(x) = (x-x_{\alpha,\ell})^2/(x_{\alpha,r}-x_{\alpha,\ell})^2 \cdot (x-x_{\alpha,r}) \\ \phi_5(x) = \phi_1(x)\phi_3(x)/(\phi_1(x_\alpha)\phi_3(x_\alpha)) \end{cases}$	$\kappa_{0,\ell}$ $\kappa_{0,r}$ $\tilde{x}_{0,\ell}$ $\tilde{x}_{0,r}$ x_0 $x_{0,\ell}$ $x_{0,r}$ $\check{w}_0$ E_0	$0.60\,\mathrm{pN\,nm^{-1}}$ $0.99\,\mathrm{pN\,nm^{-1}}$ $-2\,\mathrm{nm}$ $2\,\mathrm{nm}$ $-2\,\mathrm{nm}$ $-3.5\,\mathrm{nm}$ $0.5\,\mathrm{nm}$ $5.7\,\mathrm{zJ}$ $70\,\mathrm{zJ}$
Transitions rates (see Figure 4(b)&(c))		
Attachment rate		
$\begin{cases} k_+(x,h) = k^+_{\max}\Big[\frac{1}{2}\Big(1+\tanh\big[\lambda^+_h(h+h^+_{\frac{1}{2}})\big]\Big)\mathbb{1}_{h<0}(h) \\ \quad +\frac{1}{2}\Big(1-\tanh\big[\lambda^+_h(h-h^+_{\frac{1}{2}})\big]\Big)\mathbb{1}_{h\geq 0}(h)\Big] \\ \quad \cdot\Big[\frac{1}{2}\Big(1+\tanh\big[\lambda^+_x(x+x^+_\ell)\big]\Big)\mathbb{1}_{x<0}(x) \\ \quad +\frac{1}{2}\Big(1-\tanh\big[\lambda^+_x(x-x^+_r)\big]\Big)\mathbb{1}_{x\geq 0}(x)\Big] \end{cases}$	$k^+_{\max}$ λ^+_h $h^+_{\frac{1}{2}}$ λ^+_x x^+_ℓ x^+_r	$0.206\,\mathrm{ms^{-1}}$ $1.6\,\mathrm{nm^{-1}}$ $2.7\,\mathrm{nm}$ $1.6\,\mathrm{nm^{-1}}$ $5\,\mathrm{nm}$ $10\,\mathrm{nm}$
Reverse detachment rate		
$\begin{cases} k^{\mathrm{rev}}_-(x,h) = k^{-,\mathrm{rev}}_{\max}\cdot\frac{1}{2}\Big(1-\tanh\big[\lambda^{-,\mathrm{rev}}_x(x-x^{-,\mathrm{rev}})\big]\Big) \\ \quad \cdot\Big[\frac{1}{2}\Big(1+\tanh\big[\lambda^{-,\mathrm{rev}}_h(h+h^{-,\mathrm{rev}}_{\frac{1}{2}})\big]\Big)\mathbb{1}_{h<0}(h) \\ \quad +\frac{1}{2}\Big(1-\tanh\big[\lambda_h(h-h^{-,\mathrm{rev}}_{\frac{1}{2}})\big]\Big)\mathbb{1}_{h\geq 0}(h)\Big] \end{cases}$	$k^{-,\mathrm{rev}}_{\max}$ $\lambda^{-,\mathrm{rev}}_h$ $h^{-,\mathrm{rev}}_{\frac{1}{2}}$ $\lambda^{-,\mathrm{rev}}_x$ $x^{-,\mathrm{rev}}$	$0.60\,\mathrm{pN\,nm^{-1}}$ $0.99\,\mathrm{pN\,nm^{-1}}$ $-1.5\,\mathrm{nm}$ $1.3\,\mathrm{nm}$ $5.70\,\mathrm{zJ}$
Thermodynamics		
Drag coefficient	η	$0.097\,\mathrm{ms\,pN\,nm^{-1}}$
Temperature	T	$298\,\mathrm{K}$
ATP chemical potential	μ_{T}	$100\,\mathrm{zJ}$
Geometrical parameters		
Actin inter-site distance	d	$40\,\mathrm{nm}$

Acknowledgments

The authors wish to thank Philippe Moireau for fruitful advices and discussions.

Bibliography

[1] Vincent Bansaye and Sylvie Méléard. *Stochastic models for structured populations*, volume 16. Springer, 2015.

[2] Marco Caremani, Luca Melli, Mario Dolfi, Vincenzo Lombardi, and Marco Linari. The working stroke of the myosin II motor in muscle is not tightly coupled to release of orthophosphate from its active site. 591(20):5187–5205.

[3] Marco Caremani, Luca Melli, Mario Dolfi, Vincenzo Lombardi, and Marco Linari. Force and number of myosin motors during muscle shortening and the coupling with the release of the ATP hydrolysis products. *The Journal of Physiology*, 593(15):3313–3332, July 2015.

[4] Marco Caremani, Francesca Pinzauti, Massimo Reconditi, Gabriella Piazzesi, Ger J M Stienen, Vincenzo Lombardi, and Marco Linari. Size and speed of the working stroke of cardiac myosin in situ. *Proceedings of the National Academy of Sciences*, 113(13):3675–3680, March 2016.

[5] M Caruel and L Truskinovsky. Physics of muscle contraction. *Reports on Progress in Physics*, 81(3):036602, Feb 2018.

[6] Matthieu Caruel. *Mechanics of Fast Force Recovery in Skeletal Muscles*. PhD thesis, 10 2011.

[7] Matthieu Caruel, Philippe Moireau, and Dominique Chapelle. Stochastic modeling of chemical-mechanical coupling in striated muscles. *Biomechanics and Modeling in Mechanobiology*, 18, 06 2019.

[8] Matthieu Caruel, Philippe Moireau, and Dominique Chapelle. Stochastic modeling of chemical-mechanical coupling in striated muscles. *Biomechanics and Modeling in Mechanobiology*, 18(3):563–587, June 2019.

[9] Dominique Chapelle, Patrick Tallec, Philippe Moireau, and Michel Sorine. Energy-preserving muscle tissue model: Formulation and compatible discretizations. *International Journal for Multiscale Computational Engineering*, 10:189–, 01 2012.

[10] Pierre Del Moral and Spiridon Penev. *Stochastic Processes: From Applications to Theory* . December 2016.

[11] T. A. J. Duke. Molecular model of muscle contraction. 96(6):2770–2775.

[12] K A Edman. Double-hyperbolic force-velocity relation in frog muscle fibres. 404(1):301–321.

[13] K. A. P. Edman and NA Curtin. Synchronous oscillations of length and stiffness during loaded shortening of frog muscle fibres. 534(265):553–563.

[14] E Eisenberg and Terrell L Hill. A cross-bridge model of muscle contraction. *Progress in Biophysics and Molecular Biology*, 33(1):55–82, 1978.

[15] E Eisenberg, Terrell L Hill, and Y Chen. Cross-bridge model of muscle contraction. Quantitative analysis. *Biophysical Journal*, 29(2):195–227, 1980.

[16] T Erdmann and Ulrich Schwarz. Impact of receptor-ligand distance on adhesion cluster stability. *The European physical journal. E, Soft matter*, 22:123–37, 03 2007.

[17] A. M. Gordon, E. Homsher, and M. Regnier. Regulation of Contraction in Striated Muscle. 80(2):853–924.

[18] Carl Graham. Mckean-vlasov itô-skorohod equations, and nonlinear diffusions with discrete jump sets. *Stochastic processes and their applications*, 40(1):69–82, 1992.

[19] H. L. Granzier, A. Mattiazzi, and G. H. Pollack. Sarcomere dynamics during isotonic velocity transients in single frog muscle fibers. 259(2):C266–C278.

[20] T Guérin, J Prost, and J F Joanny. Dynamical behavior of molecular motor assemblies in the rigid and crossbridge models. *The European Physical Journal E*, 34(6):667–21, June 2011.

[21] A.V. Hill. The heat of shortening and the dynamic constants of muscle. 126(843):136–195, 1938. Publisher: The Royal Society.

[22] Terrell L Hill. Theoretical formalism for the sliding filament model of contraction of striated muscle Part I. *Progress in Biophysics and Molecular Biology*, 28:267–340, 1974.

[23] Terrell L Hill. Theoretical formalism for the sliding filament model of contraction of striated muscle part II. *Progress in Biophysics and Molecular Biology*, 29:105–159, 1976.

[24] Terrell L Hill. *Free Energy Transduction in Biology.* Academic press, 1977.

[25] Anne Houdusse and H. Lee Sweeney. How Myosin Generates Force on Actin Filaments. 41(12):989–997.

[26] Jonathon Howard and Jonathon Howard. *Mechanics of Motor Proteins and the Cytoskeleton*. Sinauer, Sunderland, MA. Sinauer Associates Incorporated.

[27] A F Huxley. Muscle structure and theories of contraction. 7:255–318.

[28] Andrew F Huxley and R M Simmons. Proposed mechanism of force generation in striated muscle. *Nature*, 233(5321):533–538, 1971.

[29] Jean Jacod and Albert Shiryaev. *Limit theorems for stochastic processes*, volume 288. Springer Science & Business Media, 2013.

[30] Frank Jülicher, Armand Ajdari, and Jacques Prost. Modeling molecular motors. 69(4):1269–1282.

[31] F. Kimmig and M. Caruel. Hierarchical modeling of force generation in cardiac muscle. *Biomechanics and Modeling in Mechanobiology*, 19(6):2567–2601, 2020.

[32] François Kimmig. *Modélisation multi-échelles de la contraction musculaire : De la dynamique stochastique des moteurs moléculaires à la mécanique des milieux continus*. Theses, Université Paris-Saclay, December 2019.

[33] François Kimmig and Matthieu Caruel. Hierarchical modeling of force generation in cardiac muscle. *Biomechanics and Modeling in Mechanobiology*, 19:2567–2601, 2020.

[34] Tomoyoshi Kobayashi, Lei Jin, and Pieter P de Tombe. Cardiac thin filament regulation. *Pflügers Archiv - European Journal of Physiology*, 457(1):37–46, 2008.

[35] Jean-François Le Gall. *Brownian motion, martingales, and stochastic calculus*. Springer, 2016.

[36] J. L. Lions and E. Magenes. *Variational Evolution Equations*, pages 227–308. Springer Berlin Heidelberg, Berlin, Heidelberg, 1972.

[37] R. W. Lymn and E. W. Taylor. Mechanism of adenosine triphosphate hydrolysis by actomyosin. *Biochemistry*, 10(25):4617–4624, 1971. PMID: 4258719.

[38] Alf Månsson. Actomyosin-ADP States, Interhead Cooperativity, and the Force-Velocity Relation of Skeletal Muscle. 98(7):1237–1246.

[39] Alf Månsson. Actomyosin based contraction: One mechanokinetic model from single molecules to muscle? 37(6):181–194.

[40] Alf Månsson. Comparing models with one versus multiple myosin-binding sites per actin target zone: The power of simplicity. 151(4):578–592.

[41] Alf Månsson. Hypothesis: Single Actomyosin Properties Account for Ensemble Behavior in Active Muscle Shortening and Isometric Contraction. 21(21):8399.

[42] Alf Månsson, Malin Persson, Nabil Shalabi, and Dilson E. Rassier. Nonlinear Actomyosin Elasticity in Muscle? 116(2):330–346.

[43] Justin E Molloy, Julie E Burns, John C Sparrow, Richard T Tregear, John Kendrick-Jones, and David C S White. Single-Molecule Mechanics of Heavy Meromyosin and Si Interacting with Rabbit or Drosophila Actins Using Optical Tweezers. 68:6.

[44] Benoît Perthame. Parabolic equations in biology. In *Parabolic Equations in Biology*, pages 1–21. Springer, 2015.

[45] Irene Pertici, Lorenzo Bongini, Luca Melli, Giulio Bianchi, Luca Salvi, Giulia Falorsi, Caterina Squarci, Tamás Bozó, Dan Cojoc, Miklós S. Z. Kellermayer, Vincenzo Lombardi, and Pasquale Bianco. A myosin II nanomachine mimicking the striated muscle. 9(1):3532.

[46] G. Piazzesi and V. Lombardi. A cross-bridge model that is able to explain mechanical and energetic properties of shortening muscle. *Biophysical journal*, 68 5:1966–79, 1995.

[47] Gabriella Piazzesi and Vincenzo Lombardi. A cross-bridge model that is able to explain mechanical and energetic properties of shortening muscle. *Biophysical Journal*, 68(5):1966–1979, 1995.

[48] Gabriella Piazzesi, Massimo Reconditi, Marco Linari, Leonardo Lucii, Pasquale Bianco, Elisabetta Brunello, Valérie Decostre, Alex Stewart, David B. Gore, Thomas C. Irving, Malcolm Irving, and Vincenzo Lombardi. Skeletal Muscle Performance Determined by Modulation of Number of Myosin Motors Rather Than Motor Force or Stroke Size. 131(4):784–795.

[49] Francesca Pinzauti, Irene Pertici, Massimo Reconditi, Theyencheri Narayanan, Ger J M Stienen, Gabriella Piazzesi, Vincenzo Lombardi, Marco Linari, and Marco Caremani. The force and stiffness of myosin motors in the isometric twitch of a cardiac trabecula and the effect of the extracellular calcium concentration. *The Journal of Physiology*, 596(13):2581–2596, May 2018.

[50] Massimo Reconditi. Recent improvements in small angle x-ray diffraction for the study of muscle physiology. 69(10):2709–2759.

[51] D. A. Smith and S. M. Mijailovich. Toward a Unified Theory of Muscle Contraction. II: Predictions with the Mean-Field Approximation. 36(8):1353–1371.

[52] D.A. Smith and M.A. Geeves. Strain-dependent cross-bridge cycle for muscle. 69(2):524–537.

[53] D.A. Smith and M.A. Geeves. Strain-dependent cross-bridge cycle for muscle. II. Steady-state behavior. 69(2):538–552.

[54] D.A. Smith, M.A. Geeves, J. Sleep, and S.M. Mijailovich. Towards a Unified Theory of Muscle Contraction. I: Foundations. 36(10):1624–1640.

[55] Walter Steffen, David Smith, Robert Simmons, and John Sleep. Mapping the actin filament with myosin. 98(26):14949–14954.

[56] H Sugi and T Tsuchiya. Isotonic velocity transients in frog muscle fibers following quick changes in load. 319:219–238.